

Protease-Sensitive Nanomaterials for Cancer Therapeutics and Imaging

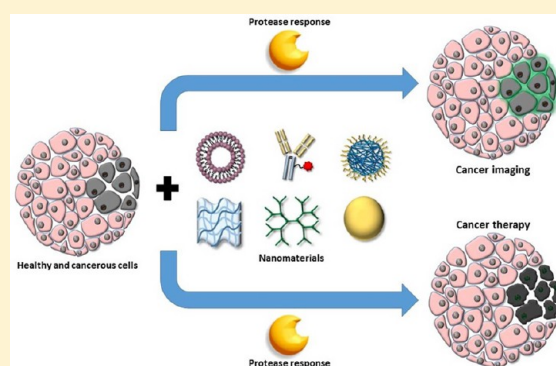
Caleb F. Anderson[†] and Honggang Cui^{*,†,‡,§}

[†]Department of Chemical and Biomolecular Engineering and Institute for NanoBioTechnology, Johns Hopkins University, 3400 North Charles Street, Baltimore, Maryland 21218, United States

[‡]Department of Oncology and Sidney Kimmel Comprehensive Cancer Center, Johns Hopkins University School of Medicine, Baltimore, Maryland 21205, United States

[§]Center for Nanomedicine, The Wilmer Eye Institute, Johns Hopkins University School of Medicine, 400 North Broadway, Baltimore, Maryland 21231, United States

ABSTRACT: Many diseases can be characterized by the abnormal activity exhibited by various biomolecules, the targeting of which can provide therapeutic and diagnostic utility. Recent trends in medicine and nanotechnology have prompted the development of protease-sensitive nanomaterials systems for therapeutic, diagnostic, and theranostic applications. These systems can act specifically in response to the target enzyme and its associated disease conditions, thus enabling personalized treatment and improved prognosis. In this Review, we discuss recent advancements in the development of protease-responsive materials for imaging and drug delivery and analyze several representative systems to illustrate their key design principles.



INTRODUCTION

Enzymatic proteins can exhibit abnormal activity in a wide variety of diseases such as cancer and autoimmune disorders and, therefore, can be exploited for therapeutic and diagnostic purposes.^{1–5} This anomalous activity can help to increase the specificity and selectivity of drugs to diseased sites to reduce the harmful consequences of impacting healthy tissues and cells. The ability to detect precisely these activities could also prove beneficial for early stage diagnosis and enable a more accurate evaluation of disease progression. Moreover, imaging of these biomolecules can provide real time information in a noninvasive manner, thus allowing the selection of the most appropriate medical treatments.⁶

Enzymes play crucial roles in the progression and spread of cancer, being involved in the processes of cancer cell growth, angiogenesis, and metastasis among others. This importance makes enzymes suitable targets for therapeutic and diagnostic purposes.^{1,7–9} There are many unique aspects of tumor physiology and pathology that can be utilized for targeting and treatment. For example, many tumor types contain leaky, irregularly shaped blood vessels that allow therapeutics and imaging probes to enter the tumor easily; poor lymphatic drainage then leads to greater retention.¹⁰ For greater selectivity, however, an *active* targeting strategy is preferred, one that provides a distinct means of distinguishing cancerous tissues from healthy. In this case, targeting of abnormally expressed enzymes could be advantageous, though there are other tumor microenvironment factors that can also be targeted

for improved selectivity, including pH,^{11,12} cell-surface receptors,^{13,14} redox potential,¹⁵ hypoxia,¹⁶ and more.^{17,18}

Enzymes are relevant and effective targets for selective cancer drug and imaging probe delivery due to their substrate specificity and ability to perform biological catalysis.^{4,19,20} A wide variety of enzyme classes are overexpressed in tumor microenvironments, such as proteases, lipases, oxidoreductases, and phosphatases, and serve as potential targets,^{3,21} however, our focus here will center on cancer-associated proteases. The proteases that can be used for cancer therapy and imaging are cathepsins,^{22,23} matrix metalloproteinases,^{24,25} caspases,⁹ and urokinases.^{7,19,26} With a specific protease in mind, responsive drugs and imaging probes can be designed for that target to increase selectivity and efficacy.

Nanomaterials have been used for various medicinal applications and have made a significant impact on the field of drug delivery and diagnosis by improving efficacy and reducing systemic toxicity.^{4,27} A wide variety of platform nanostructures and materials have been developed,^{3,28} including liposomes,²⁹ dendrimers,³⁰ inorganic nanoparticles,^{31–33} hydrogels,^{34–36} protein conjugates,³⁷ and polymeric nanoparticles.^{38–40} Several key design features impact their pharmacokinetic profiles and biodistribution, such as shape, size, and surface chemistry, and must be considered when

Received: March 8, 2017

Revised: April 14, 2017

Accepted: April 24, 2017

Published: April 24, 2017

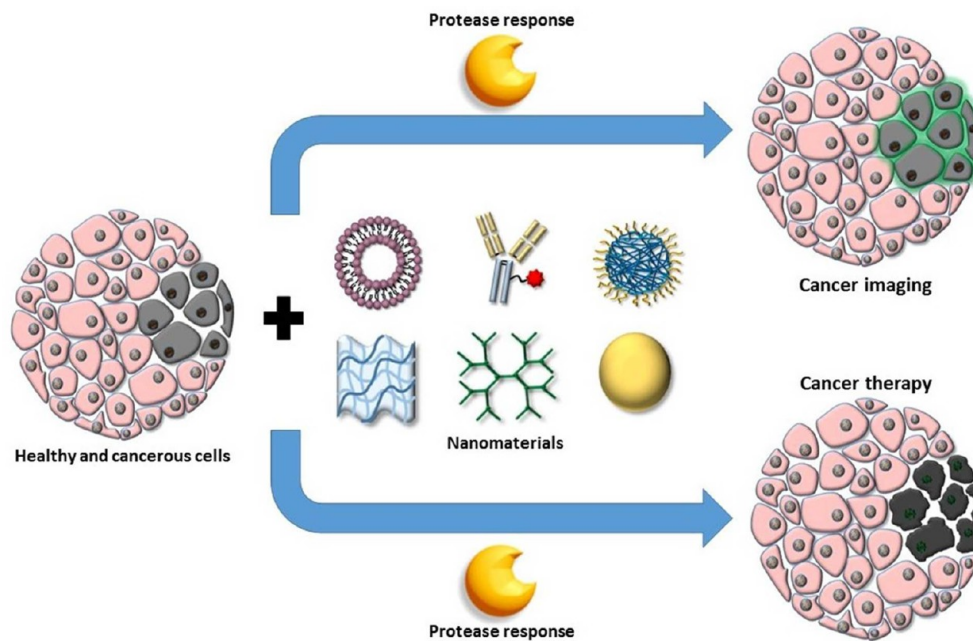


Figure 1. Tissues containing healthy (pink) and tumor (gray) cells can be treated with various nanomaterials, such as (from left to right) liposomes, protein-conjugates, polymeric nanoparticles, hydrogels, dendrimers, and inorganic metal nanoparticles, to deliver imaging agents or anticancer drugs with improved selectivity to tumor cells by incorporation of protease-responsiveness into the design of nanomaterials.

developing new nanomedicines.^{41–46} Specifically, in cancer imaging and treatment, nanomaterial-based systems offer many advantages over small molecule drugs and imaging probes. Nanomaterials have greater solubility and stability *in vivo* with longer circulation times and slower clearance rates that allow for sustained delivery. With their ability to be engineered for particular stimuli-responsiveness, enhanced accumulation in tumors, and high loading capacity from high surface-area-to-volume ratios, nanomaterials serve as ideal candidates for combating cancer.^{44,47} Certain nanomaterials can also be formed from self-assembling monomers, offering further advantages by simplifying formulation and development through the reduction of unnecessary components.^{44,47} Nanomaterials can be designed to interact with enzymes to induce self-assembly or to trigger drug release within the confines of the tumor(s), which can improve targeting efficacy and reduce unwanted signals or side-effects in healthy tissues.^{48–50}

Some nanomaterials have found utility in medicine as imaging probes activatable by proteases, whereby enzymatic cleavage turns the probes “on” to yield a detectable signal.^{6,51,52} This concept is illustrated in Figure 1. Protease-activated materials have been applied to a wide variety of imaging techniques for disease detection, such as optical/fluorescence imaging, magnetic resonance imaging (MRI), nuclear imaging (PET, SPECT, and CT), and more.^{49,53–55} Recent efforts have pushed for the development of imaging probes with multiple modalities to benefit from the advantages each component offers for more accurate signaling.⁵⁶ Using protease-sensitive nanomaterials for molecular imaging can improve overall accuracy by enhancing target-site accumulation, increasing detectable signals via enzymatic cleavage, improving resistance to nonspecific degradation, and accelerating clearance from the body to reduce background noise. For cancer, these nanomaterial-based probes can present precise information for early detection, staging, diagnosis, and response monitoring to improve patient care.⁵⁵

The benefits of using protease-responsive nanomaterials for imaging directly translate to efficacious drug delivery,¹ which is also illustrated in Figure 1. In recent years, trends in nanomedicine have been for the development of theranostic agents that are capable of simultaneous or tandem diagnosis and therapy.^{27,28,57} The combination of imaging and therapeutic capabilities in a nanomaterial-based delivery system offers advantages over imaging and therapeutics alone, with minor trade-offs that can be mitigated by incorporating protease-sensitivity into its design. Theranostic probes can reveal when and how drugs are delivered and allow for monitoring of a patient’s response to therapy. From the information obtained by directly visualizing the pharmacokinetics of these agents, it can assist healthcare providers in decision-making by revealing optimal therapeutic strategies for that specific patient, paving the way toward personalized medicine in the future. Using nanomaterial-based systems as theranostic agents can improve therapeutic efficacy, mitigate off-target toxicity, and ultimately lead to better patient outcomes. Integrating protease-sensitivity improves selective accumulation and activation at diseased sites and can help overcome the trade-offs between the different time scales needed for imaging and therapeutics. Molecules with intrinsic duality are ideal candidates, as they are simpler to synthesize and do not have to compromise on the extent of loading between the imaging agent and the drug.^{57–62}

In this Review, we will discuss recent advances in imaging and drug delivery with protease-responsive nanomaterials for cancer with a focus on theranostic systems, paying particular attention to their molecular design. Since there has been a conscious effort in nanomedicine to design systems sensitive to multiple environmental stimuli for improved selectivity and signal ratios,^{13,16,63} our discussion will also include systems that incorporate responsiveness to other tumor microenvironment factors in conjunction with protease sensitivity.

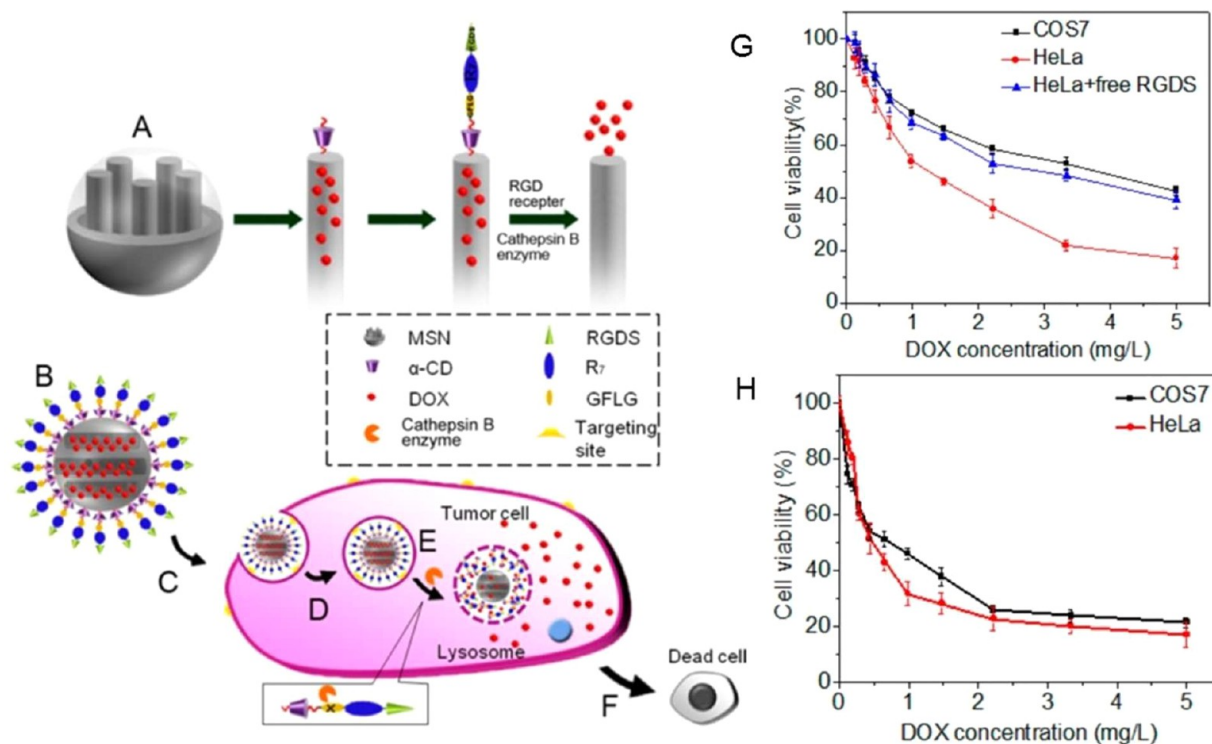


Figure 2. (A–F) Functionalization procedure and mechanism of action of the doxorubicin-loaded mesoporous silica nanoparticles (MSNs), where panel A shows capping of and subsequent release from the MSNs of doxorubicin, panel B shows the drug-loaded MSNs as they appear in physiological pH, panel C illustrates targeting to $\alpha_v\beta_3$ integrins overexpressed on cancer cells by the RGDS peptide sequence, panel D portrays endocytosis of MSNs into a specific tumor cells, panel E shows triggered drug release by cathepsin B activity, and panel F represents the tumor cell undergoing apoptosis. (G) Cell viability data of COS7 and HeLa cells incubated *in vitro* with doxorubicin-loaded MSN-GFLGR_rRGDS/ α -CD in the absence or presence of free RGDS peptide (2 μ M) and (H) free doxorubicin, highlighting the comparable cytotoxicity as the free drug but with more specificity to tumor cells. Adapted with permission from ref 72. Copyright 2015 American Chemical Society.

■ PROTEASE-RESPONSIVE NANOMATERIAL SYSTEMS FOR THERAPEUTICS

Nanomaterials have been widely employed for the improvement of already commercially available anticancer therapeutics, where their ability to improve drug solubility and retention in tumors has helped increase efficacy and safety.^{16,33,40,41,44,64,65} Incorporation of protease sensitivity can further improve selectivity to tumor tissue and mitigate harmful side effects to healthy tissues.^{66–69} Of particular interest are the following proteases whose abnormal activity is associated with cancer: cathepsins, matrix metalloproteinases, and urokinase-type plasminogen activators. Cathepsins are lysosomal cysteine proteases that play a role in regulating angiogenesis during cancer progression and in initiating and promoting tumor formation, growth, invasion, and metastasis.^{22,23} Matrix metalloproteinases (MMPs) are extracellular zinc-containing extracellular matrix (ECM) endopeptidases that play a role in tumor growth, invasion, and metastasis.²⁴ The urokinase-type plasminogen activator (uPA) is a serine protease and a member of the uPA system on the cell surface; uPA degrades the ECM and activates its substrate plasmin, which is more destructive. Its activity plays a role in enhancing cell migration, invasion, and metastasis.⁷⁰ Although proteases are most often utilized to release drugs from nanomaterial carriers, recent studies have investigated using proteases for inducing formation of nanostructures that may be cytotoxic to cancer cells themselves or to change the shape or size of nanocarriers to impact drug release profiles.²¹ In this section, we will discuss recent studies on the design of protease-responsive nanomaterials that release

drug cargo or aggregate in tumor microenvironments to yield therapeutic effects, including some examples of systems responsive to other additional microenvironment factors.

Protease-Responsiveness for Cargo Release. In one example, Bossmann and co-workers worked to develop a protease-sensitive liposome that would address common problems faced by liposome carriers, such as decreasing the amount of leaking from the vesicles, increasing their release kinetics, and being able to target cancer cells more specifically.⁷¹ The liposomes were designed with a cholesterol-anchored, graft copolymer containing a uPA-cleavable peptide sequence (SGRSA) and poly(acrylic acid), and the liposomes used have high osmolarities to make them swell more easily. The liposomes are cross-linked with diamine and ethylenediamine, which causes the liposomes to exhibit significantly increased resistance to osmotic swelling and thus prevents premature leaking of their contents. In the presence of uPA, these liposomes are able to deliver their entire payload, indicating their heightened sensitivity to the protease. The focus of this study was on creating and optimizing the design of these liposomes, so no *in vitro* or *in vivo* studies were conducted. An optimal design was created by looking at the impact of cross-linking level and degree of polymer-incorporation on release against osmotic pressure, showcasing the numerous factors and importance of nanomaterial design to be efficacious for drug delivery.⁷¹

In another example, He and co-workers developed a mesoporous silica nanoparticle (MSN) to improve the targeting of the anticancer drug doxorubicin (Dox) to cancer cells while

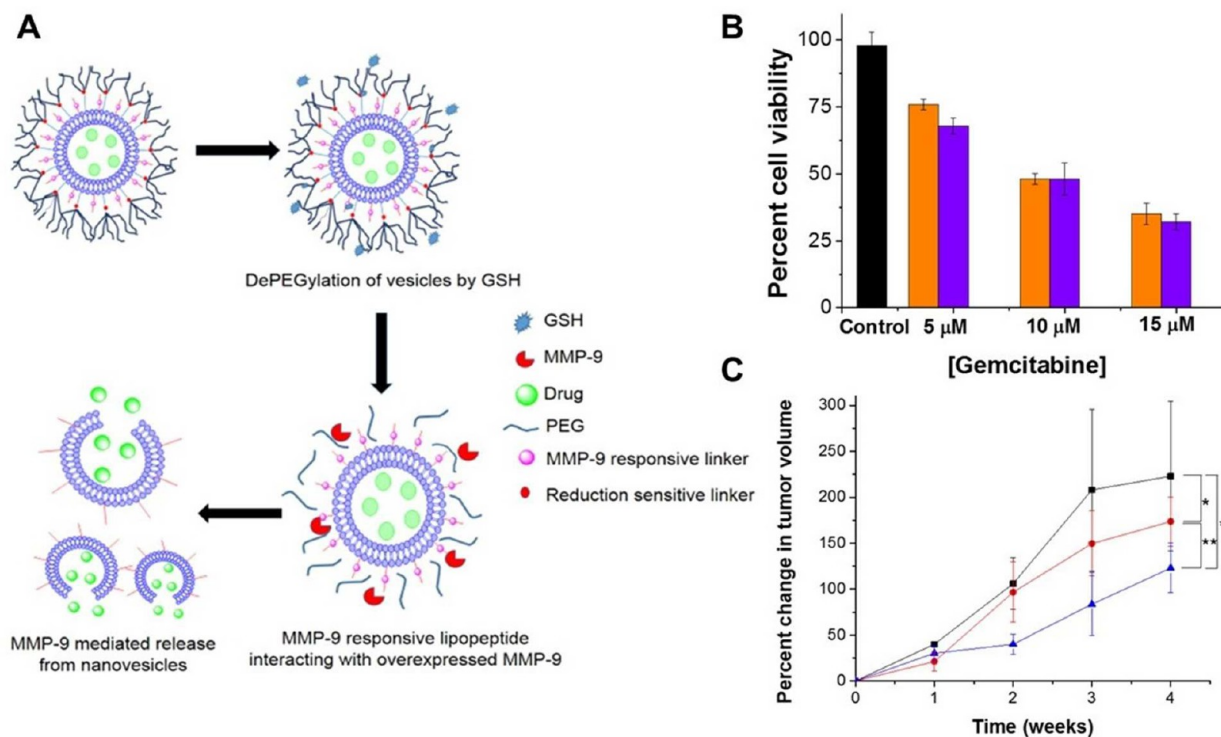


Figure 3. (A) Illustration of nanovesicles and their targeting mechanism that are responsive to the elevated levels of extracellular GSH and MMP-9 by incorporating MMP-9 substrate lipopeptides and reduction-sensitive POPE-SS-PEG on their surface. (B) *In vitro* cell viability data showcasing the concentration dependent decrease in MIA PaCa-2 cell viability when treated with free gemcitabine (violet) or gemcitabine-loaded nanovesicles (orange) for 72 h. (C) Tumor volume percentage increase from xenograft mice model, where blue represents test group ($n = 3$) treated with MMP-9 substrate-incorporated nanovesicles, red represents group ($n = 3$) treated with nanovesicles without MMP-9 responsiveness, and black is the control group ($n = 3$) treated with PBS-loaded nanovesicles (* $p < 0.05$, ** $p < 0.05$). Adapted with permission from ref 74. Copyright 2014 American Chemical Society.

reducing adverse side effects to healthy cells.⁷² MSNs are suitable drug carriers because they have a large loading capacity, are easily functionalized, have low toxicity, and are chemically inert. This design involves a classic rotaxane structure formed between an alkoxysilane tether and α -cyclodextrin (α -CD) used to anchor onto orifices of MSNs and act as gatekeeper for doxorubicin release. These are modified with a multifunctional peptide (azido-GFLGR₇RGDS) that contains $\alpha_v\beta_3$ integrin (overexpressed on the surfaces of different cancer lines) targeting sequence RGDS, cell penetrating peptide sequence R₇, and cathepsin B-cleavable peptide sequence GFLG, which function to penetrate tumor cells selectively and release doxorubicin. Figure 2 showcases the design of these MSNs and their mechanism of action. Drug release behavior studies with nanoparticles in PBS showed that the nanoparticles had the greatest release of contents in the presence of cathepsin B at lysosomal pH, indicating the requirement of cathepsin B cleavage for sufficient drug delivery. *In vitro* studies were conducted with $\alpha_v\beta_3$ -positive HeLa cancer cells that overexpress cathepsin B and $\alpha_v\beta_3$ -negative COS7 cells that express cathepsin B at relatively low levels. These studies showed higher uptake in HeLa cells but lower cytotoxicity than free doxorubicin, as shown in Figure 2, by flow cytometry and MTT assay. The difference in cytotoxicity between the MSNs and free Dox is likely due to the slower rate of endocytosis of the MSNs as opposed to concentration gradient diffusion by free Dox; however, the MSNs have an increased selectivity from $\alpha_v\beta_3$ -targeting and cathepsin B-triggered drug release that makes them safer alternatives to the free drug. The difference in cell viability between HeLa cells, $\alpha_v\beta_3$ receptor-blocked HeLa

cells, and COS7 cells highlights the selectivity of the $\alpha_v\beta_3$ - and cathepsin B-targeting motifs of the MSNs. Although no *in vivo* study has been conducted with these MSNs, this study highlights the advantages of targeting other tumor micro-environment factors (specifically receptor overexpression) in conjunction with protease overexpression for improving the selectivity of drug delivery and release to cancer cells over healthy cells.⁷²

In another example with multiresponsiveness, Jiang and co-workers developed a nanoparticle system responsive to both extracellular pH and MMP-2 activity for gene delivery.⁷³ Their design involves dendrigraft poly lysine (DGL) that complexes and condenses DNA to form a nonviral vector nanoparticle via electrostatic interactions. The nanoparticles are modified with a dual-triggered activatable cell-penetrating peptide (dtACPP), composed of a pH-sensitive masking peptide (e_4k_4 , D-amino acids, pI = 6.4), an MMP-2 substrate (PLGLAG), and a polycationic cell-penetrating peptide (nonarginine). The dtACPPs are conjugated to the surface of a DGL via α -maleimidyl- ω -N-hydroxysuccinimidyl polyethylene glycol (MAL-PEG-NHS) to create the gene nanocarrier, dtACPP-PEG-DGL (dtACPPD). The internalization of the nanoparticles via the cell-penetrating peptide is inhibited until the nanoparticles enter environments with pH values typical of tumors; here the now positively or neutrally charged pH-sensitive masking peptide can be cleaved by overexpressed MMP-2 to then enhance cellular uptake of the genes to cancer cells. Cytotoxicity of the dtACPPDs was tested using flow cytometry and fluorescent microscopy with BEL-7402 hepatocellular carcinoma cells cultured at either pH 6.0 or 7.4 and

pretreated with or without MMP-2, showing uptake as high as 90.6% in the presence of MMP-2 at a pH of 6.0 (mimicking slightly acidic tumor microenvironment). *In vivo* testing with mice showed progressive accumulation of dtACPPDs in tumors over time with the smallest accumulation in liver and kidneys in comparison to different control groups. This study further showcases the benefits of multiresponsive targeting to cancer cells and how its incorporation into nanocarrier design can improve overall therapeutic efficacy.⁷³

In a study by Mallik and co-workers, they designed nanovesicles responsive to overexpression of glutathione (GSH) and MMP-9 in the tumor microenvironment to deliver efficiently and selectively the anticancer drug gemcitabine (Gem).⁷⁴ An MMP-9-cleavable, collagen mimetic lipopeptide forms nanovesicles with 1-palmitoyl-2-oleoyl-*sn*-glycero-3-phosphocholine (POPC), cholesteryl-hemisuccinate, and the reduction-sensitive, PEGylated 1-palmitoyl-2-oleoyl-*sn*-glycero-2-phosphethanolamine lipid (POPE-SS-PEG₅₀₀₀). The PEGylation helps instill long circulating characteristics to the nanovesicles while also reducing unintended interactions with circulating proteins. Once at cancer sites, the PEG chains are shed via reduction by GSH, which then exposes the vesicle to MMP-9 degradation, allowing for release of the contents inside. The design and mechanism of release are detailed in Figure 3. *In vitro* cytotoxicity was investigated with PANC-1 and MIAPaCa-2 pancreatic cancer cells of Gem-loaded nanovesicles, showing lower cell viability with the PANC-1 line (30–35%), which has a higher expression of MMP-9 than MIAPaCa-2 (viability 45–50%), where dose-dependent cytotoxicity evidence is shown in Figure 3. In a spheroid culture, the cell viability was similar between free and encapsulated Gem in PANC-1 cells, showing encapsulation does not compromise cytotoxicity while simultaneously improving selectivity. An *in vivo* xenograft mice model with PANC-1 cancer cells showed a more significant reduction in tumor growth for the Gem-encapsulated, MMP-9-responsive nanovesicles in comparison to vesicles without an MMP-9 substrate in their design, which can be seen in Figure 3. The difference in tumor growth and the fact that animals remained healthy after treatment illustrates better control of Gem release with MMP-9 selectivity, highlighting another case where multiresponsiveness significantly improves selectivity to cancer cells.⁷⁴

Protease-Responsiveness for Nanostructure Formation. Although proteases are often targeting to trigger drug release from various nanomaterials, recent work has been done for the development of nanomaterials systems that use proteases to trigger nanostructure formation to change drug release kinetics or to induce cytotoxicity by their assembly. Maruyama and co-workers detail their design of a gelator precursor that undergoes intracellular self-assembly to form nanofibers, leading to hydrogelation and inducing cancer cell death after interacting with MMP-7.⁷⁵ The gelator precursor, *N*-palmitoyl-GGGHGPLGARK-CONH₂ (called ER-C16), design incorporated a 16-carbon alkyl chain to provide hydrophobic interactions to enhance self-assembly in aqueous solutions attached to a peptide sequence containing the following: the tetrapeptide sequence GGGH to facilitate assembly as a hydrogen-bond acceptor and donor, the MMP-7-cleavable tetrapeptide sequence PLGL for triggering gelation, and the cationic peptide sequence RK to prevent ER-C16 from forming nanofibers until cleaved off by MMP-7. From TEM imaging, the group found that the gelator precursor forms

micelle-like structures until exposed to MMP-7 which initiates self-assembly to nanofibers. The cytotoxicity of ER-C16 was investigated *in vitro* with HeLa cancer cells and MvE normal human microvascular endothelial cells, where their coculture with exposure to ER-C16 confirmed its selectivity to cancer cells due to increased uptake in HeLa cells. The decreased levels of cell viability confirmed the relationship between cell death and high intracellular toxicity and provides a therapeutic strategy that cancer cells are unlikely to acquire drug resistance to, highlighting a different but effective use of nanomaterials to selectively target and treat cancer.⁷⁵

Xu and co-workers have been exploring the concept of enzyme-instructed self-assembly for therapeutics for the past few years, developing a peptide-based system that responds to alkaline phosphatase for the formation of hydrogels.⁷⁶ Their earlier design involves the conjugation of the anticancer drug taxol to a succinic acid linker to attach the phosphatase substrate and self-assembly motif (NapFFKYp) to form a hydrogelator precursor.⁷⁷ After exposure to enzyme activity, the precursors self-assemble into nanofibers and form a supramolecular hydrogel of the taxol derivative, instilling the dual role of delivery vehicle and therapeutic to this molecule. An *in vitro* study with HeLa cancer cells was conducted and showed comparable cytotoxicity between the precursor and free taxol. Taxol activity is conserved within the hydrogel and the concentration of the precursor molecule can be used to control the release rate.⁷⁷ In a more recent example of their work, Xu and co-workers demonstrated the importance of precursor design for enzyme-instructed self-assembly (EISA) for selective killing of cancer cells.⁷⁸ In this study, they designed and synthesized two different D-tetrapeptides (ffyy and analogues) containing one or two phosphotyrosine residues capped with a naphthyl group, where dephosphorylation causes the peptides to self-assemble into nanofibers in water and the use of D-amino acids prevents endogenous protease degradation. The NapFF and NapF are residues with great self-assembly promoting motifs because of aromatic–aromatic interactions, and the tyrosine residues provide a site for mono- or diphosphorylation to explore the effect of multiple enzymatic triggers on selectivity. TEM images showed that the monophosphorylated precursors form nanofibers better due to less solubility than the diphosphorylated precursors and that the peptide sequence fyfy has a higher tendency to self-assemble. *In vitro* cytotoxicity studies were conducted with HeLa cervical cancer cells and Saos-2 osteosarcoma cells that showed that precursors inhibited growth of both cell lines by EISA, but response to precursors was dependent on expression levels of alkaline phosphatase and mechanism of cell death was dependent on the cell line. Although this lab presents an example of EISA using phosphatases, it highlights the utility of nanomaterials, the importance of their design factors, and the variety of other enzymatic targets that can be used for increasing selectivity to cancer cells.⁷⁸ This strategy offers an effective means of overcoming drug resistance and treating multiple cancer lines.⁷⁹

In another example, Ulijn and co-workers demonstrated the use of proteases to induce a morphological change in nanostructures from micelles to nanofibers to impact drug release rates.⁸⁰ In their initial design, the nanostructures were loaded with the anticancer drug doxorubicin (Dox), and contained the following units: a self-assembly motif for formation of nanofibers that provides a hydrophobic binding region for drug candidates (phenylacetyl-FFAG), an MMP-9-cleavable sequence, and a hydrophilic peptide sequence (LDD)

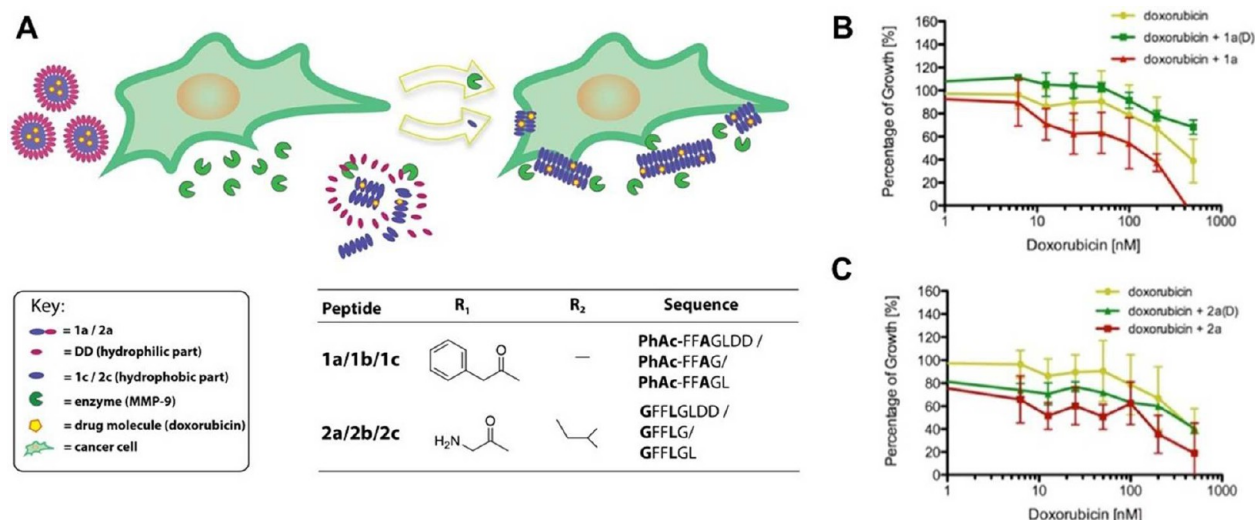


Figure 4. (A) Schematic depiction of the micelle-to-fiber transition the peptide precursors undergo due to the overexpression of MMP-9 by cancer cells, where the anticancer drug doxorubicin is entrapped in the fibrillar structures, thereby creating less mobile depots of the drug. The table represents the different peptide molecules tested in this study. (B and C) Impact of peptide design and MMP-9 responsiveness on cancer cell growth of MDA-MB-231-luc-D3H2LN cells using peptides 1a and 2a (as shown in panel A) with 2.5 mM peptides \pm 200 nM doxorubicin. Adapted with permission from ref 81. Copyright 2016 Elsevier Ltd.

that favors formation of micelles. MMP-9 cleaves off the hydrophilic unit of PhAc-FFAGLDD and confers the micelles into fibers by changing the balance between hydrophobic and hydrophilic interactions, allowing for localized and sustained delivery of Dox to cancer cells.⁸⁰ They also developed a peptide-based design (GFFLGLDD) that has the same properties as their first design for the reconfiguration of Dox-loaded micelles to nanofibers,⁸¹ and both designs are detailed in Figure 4. The reconfiguration of micelles to fibers via MMP-9 hydrolysis was confirmed with AFM and TEM for both precursor designs, and aggregation was not impacted by the presence of Dox. An *in vitro* study was conducted with MDA-MB-231-luc-D3H2LN breast cancer cells that showed significantly reduced cell viability following treatment with both precursors but slightly lower with the peptide-based design (35% vs 37.5% viability, data shown in Figure 4), and confocal microscopy confirmed uptake of drug by presence of aggregates in cytoplasm and nucleus of cells with larger aggregates outside cells, indicating local and sustained delivery were possible and effective with these precursor molecules. The same cancer cells were used for a xenograft mice model for *in vivo* efficacy studies, which further validated the selectivity and efficacy of the system for localized and sustained delivery of Dox.⁸¹ This study exemplifies the wide-ranging utility of nanomaterials for cancer therapy and highlights the role proteases can play in formation of nanostructures to control drug release, similar to the other works mentioned in this section.

■ PROTEASE-RESPONSIVE NANOMATERIAL SYSTEMS FOR DIAGNOSTICS

Extensive work has been conducted over the past decade on the development of molecular probes with sensitivity to proteases overexpressed in cancer cells.^{51,52,82–85} The following proteases whose abnormal activity is associated with cancer or whose activity is an indicator of cell death are of particular interest: cathepsins, matrix metalloproteinases, urokinase-type plasminogen activators, and caspases. Cathepsins, MMPs, and uPA were discussed in the previous section for their use in

therapeutics, but this can directly translate for targeting with imaging agents. Caspases are cysteine-aspartic proteases whose activity is involved in apoptosis and inflammation and therefore can be utilized as means of visualizing drug activation and efficacy.⁸⁶ A wide variety of imaging modalities can be used in cancer diagnostics, such as fluorescence imaging, MRI, and PET, each offering their own advantages.⁵³ However, different imaging techniques do possess their own limitations, and thus different nanomaterial systems have been designed to incorporate more than one modality, allowing for more holistic and accurate imaging.⁴² In this section, we will discuss various nanomaterial systems sensitive to these proteases that use various modalities for the imaging and diagnosis of cancer.

Matrix Metalloproteinase-Sensitive Systems. Matrix metalloproteinases (MMPs) are popular targets for cancer imaging due to their overexpression in many cancer types and easy accessibility based on their location on and around cell surfaces. Various imaging modalities have been incorporated into MMP-detectable systems, and utilization of nanomaterials have improved the efficacy of these systems. For example, NIR FRET-based probes conjugated to gold nanoparticles as a fluorescence quencher have been shown to be effective in detection of MMPs and could be used for early diagnosis of cancer.⁸⁷ Recent examples of MMP-responsive nanomaterial systems are highlighted here.

A novel signal-amplifiable self-assembling ¹⁹F NMR/MRI probe was developed by Hamachi and co-workers for imaging MMP-2 activity, where there is no observable signal when the probes are aggregated as nanoparticles but enzyme cleavage-induced disassembly turns the signal “on”.⁸⁸ The probe itself is composed of an MMP-2 substrate peptide (GPLGVRG), with the ¹⁹F NMR imaging moiety (3,5-bis(trifluoromethyl)benzene) attached to a lysine residue at the C-terminal end and a hydrophobic dodecyl (C₁₂) chain on the N-terminal end. The self-assembly into nanoparticles helps resolve issues concerning low sensitivity and poor delivery, whereas the ¹⁹F MRI modality has high NMR sensitivity with no background noise *in vivo*, making this a seemingly effective design for tumor

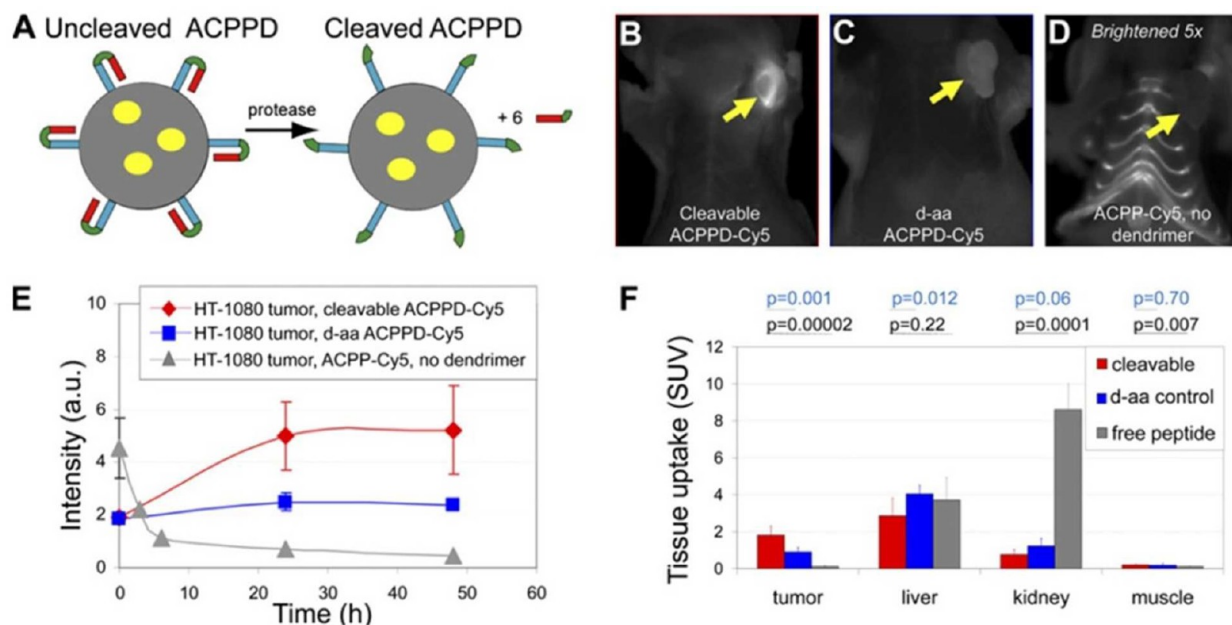


Figure 5. (A) Schematic illustration of the activatable cell-penetrating peptide dendrimer (ACPPDs), consisting of a dendrimer (gray circle) covalently attached to the polycationic segments (blue) of the ACPPs, an MMP-2,-9 cleavable peptide linker, and polyanionic segments (red) that are released to allow entry of ACPPDs into cells. The payloads stored inside the dendrimers (yellow ovals) can be either Cy5 (ACPPD-Cy5), Gd-DOTA (ACPPD-Gd), or both (dual ACPPD). (B–D) Fluorescence images taken 48 h after injection into mice (with skin removed) with ACPPD-Cy5 or ACPP-Cy5, containing 10 nmol Cy5 each, where yellow arrows point to tumors and panel D has been brightened to make signal visible, showing enhanced signal from ACPPDs over dendrimers without MMP-sensitivity and the free probe. (E) Time course of fluorescence signals in tumors in mice viewed through intact skin, demonstrating enhanced fluorescence signal of MMP-sensitive ACPPDs. (F) Standardized uptake values in solubilized samples of tumor, liver, kidney and muscle 48 h after ACPPD-Cy5 injection and 6 h after ACPP-Cy5 injection with pairwise *P* values shown for each organ type. Adapted with permission from ref 94. Copyright 2010 National Academy of Sciences.

imaging. The probes showed *in vitro* efficacy with cancer lines known to secrete MMP-2, but the ^{19}F MRI modality proved to not be as sensitive as available ^1H MRI probes, such as those that are gadolinium-based.⁸⁸

Another example of a nanoparticle system was developed by Liu and co-workers, consisting of a novel activatable photoacoustic nanoprobe for *in vivo* imaging of cancer-associated MMPs.⁸⁹ The probe is composed of an NIR-absorbing copper sulfide (CuS) nanoparticle connected to a black hole quencher (BHQ-3) via an MMP-cleavable peptide linker (GPLGVRGKGG), and showed *in vitro* reactivity to MMP-13. The BHQ-3 molecule and the CuS nanoparticle have different absorbance peaks, and comparing signals at these wavelengths can yield photoacoustic imaging of MMP activity. In a mouse model, the nanoparticles are able to detect SCC7 breast cancer cells with *in vivo* photoacoustic imaging, which in comparison to optical imaging, the mechanism of photoacoustic imaging offers distinctly improved *in vivo* spatial resolution and exhibits significantly improved tissue penetration. This system offers an interesting and unique design for an alternative imaging modality to optical fluorescence and presents its own advantages for tumor detection and imaging.⁸⁹

Over the past decade, Tsien and co-workers have been working on the development of molecular probes for the detection of MMP activity in tumors.⁹⁰ The basis of their design is the incorporation of cell-penetrating peptides (CPPs), which are integral for overcoming multidrug resistance in tumor cells.^{91,92} In their early design, their molecular probe comprised of a polyarginine-based CPP (called activatable CPPs), blocked by an inhibitory peptide sequence with negative charges, and a linker between these two domains,

which when cleaved by MMP-2 or MMP-9, allows for the CPP and its cargo, a far-red fluorophore, Cy5, to enter cancer cells. This design showed early promise with great *in vivo* contrast ratios and elevated standard uptake values in tumors relative to normal tissue in HT-1080 cancer in mice.⁹⁰ Further studies showed that these probes can target many xenograft tumor models from different cancer sites and that background uptake into normal tissue could be decreased by attaching inert macromolecules, sparking an investigation into nanomaterial conjugates.⁹³

The group developed dendrimeric nanoparticles coated with their activatable CPPs labeled with either Cy5 for fluorescence imaging, gadolinium for MRI, or both.⁹⁴ The peptide sequence, PLDLAG, serves as the MMP-cleavable linker, where cleavage separates the inhibitory domain from the loaded, CPP-conjugated polyamidoamine (PAMAM) dendrimer nanoparticle. The schematic of the nanoparticles, *in vivo* fluorescence images, and time-dependence and biodistribution data are detailed in Figure 5. The nanoparticles had significantly higher uptake in tumors than the activatable CPPs alone, allowed for fluorescence detection of tumors as small as 200 μm , and deposited high levels of Gd in tumors yielding MRI T_1 contrast that lasts several days after injection. The nanoparticle conjugation reduces background noise and improves uptake into tumor cells. Loading of the dendrimer nanoparticles with MRI and fluorescence imaging modalities improves its utility by giving it the advantages of both techniques, finding uses in MRI-guided staging and fluorescence-guided resection for many different cancer types in various parts of the body.⁹⁴ The group has also applied this nanotechnology to the MRI and fluorescence imaging of atherosclerosis and stroke with

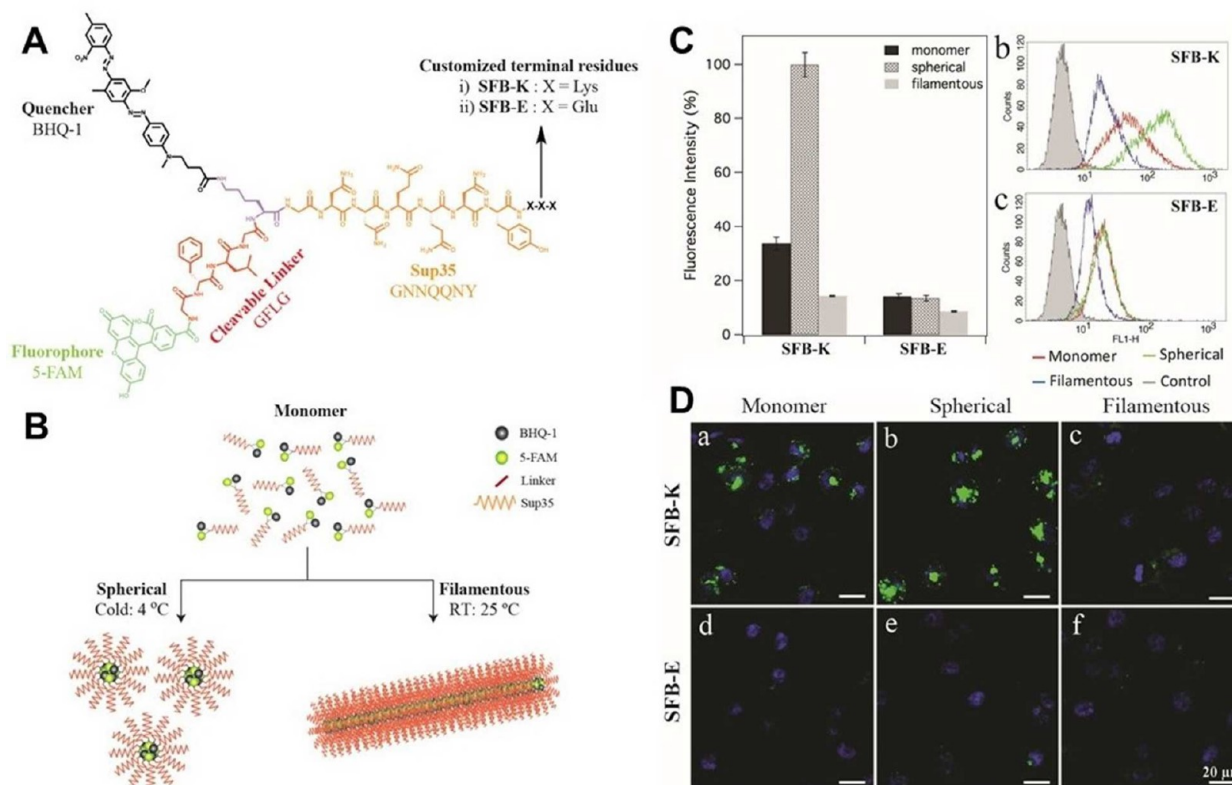


Figure 6. (A) Molecular design of the two studied molecular beacons capable of self-assembling, SFB-K and SFB-E, which are composed of the following design elements: the Black Hole Quencher-1 (BHQ-1), the fluorophore 5-FAM, the degradable peptide linker for cathepsin B specificity GFLG, and the central assembly regulating sequence GNNQQNY terminated with either three lysine (K) or glutamic acid (E) residues. (B) Schematic illustration of molecular beacons' assembly into spherical or filamentous supramolecular nanobeacons based on assembly temperature and incubation time. (C) Cellular uptake efficiency by cancer cells of beacons, varying in surface charge, shape, and assembly state, as characterized by flow cytometry: fluorescence intensity measurements (left), flow cytometry spectra comparing fluorescence intensity of SFB-K (top right) and SFB-E (bottom right). (D) Confocal laser scanning microscopy of PC3-Flu cells after 1 h incubation with 5 μM nanobeacons with different surface charges and shapes (a–f). Adapted with permission from ref 101. Copyright 2016 American Chemical Society.

different enzyme targets, and incorporated integrin $\alpha_v\beta_3$ -targeting in addition to MMP-2 sensitivity for improved sensitivity and selectivity of their probe, showcasing the ubiquity of protease-responsive nanomaterials in the imaging of many diseases.^{8,95–97}

Cathepsin-Sensitive Systems. Many groups have conducted work over the past decade exploring the development of cathepsin-sensitive probes. Many probes have incorporated various imaging modalities, such as optical imaging with fluorescence resonance energy transfer (FRET)-based probes or magnetic resonance imaging, and later have been combined with nanomaterials to improve signal ratios and targeting.^{22,82,98}

Molecular probes with cathepsin-sensitivity designed by some groups have showed a lot of potential for clinical applications. Very recently, the laboratories of Kirsch and Brigman have developed a near-infrared FRET-based probe with sensitivity to various cathepsins, particularly cathepsin S, that have progressed to *ex vivo* first-in-human phase I clinical trials in patients with soft tissue sarcoma or breast cancer.⁹⁹ Showing that their probe design is safe for use in humans and yields tumor-specific fluorescent signals, these probes could very well make it to a clinical setting. This design, however, lacks the advantages offered by nanomaterials, and successful completion of clinical trials could suggest nanomaterial systems may be just as effective for cancer imaging, if not more.

Another recent example of a cathepsin-responsive nanomaterial system was developed by Cui and co-workers, comprised of molecular probes that self-assembles into a supramolecular structure they called nanobeacons.¹⁰⁰ Their nanobeacons are comprised of hydrophobic and hydrophilic domains, where the amphiphilic nature helps to induce the self-assembly of the probes into core–shell micelles in aqueous environments. The hydrophobic domain consists of a fluorescent green dye, 5-carboxyfluorescein (5-FAM) and a black hole quencher, BHQ-1, whereas the hydrophilic domain consists of an HIV-1 derived cell-penetrating peptide sequence, Tat_{48–60}, where the charged residues allow the nanobeacons to be responsive to changes in pH. The fluorophore and quencher are held in close proximity for FRET by a cathepsin B (CatB) cleavable linker (GFLG sequence). The imaging modality is contained within the nanobeacon after spontaneous assembly into micelles and thus protected from CatB cleavage, until the nanobeacons are converted back to their monomeric form by pH or dilution to below its critical micellization concentration (CMC). The nanobeacons proved effective after incubation with MCF-7 human breast cancer cells *in vitro*, where confocal imaging and flow cytometry showed localization of the fluorescence signal in lysosomes and an increasing signal over time.¹⁰⁰

The group continued studying their nanobeacons by investigating the role that their shape and surface chemistry play on their uptake and activity *in vitro*.¹⁰¹ This design

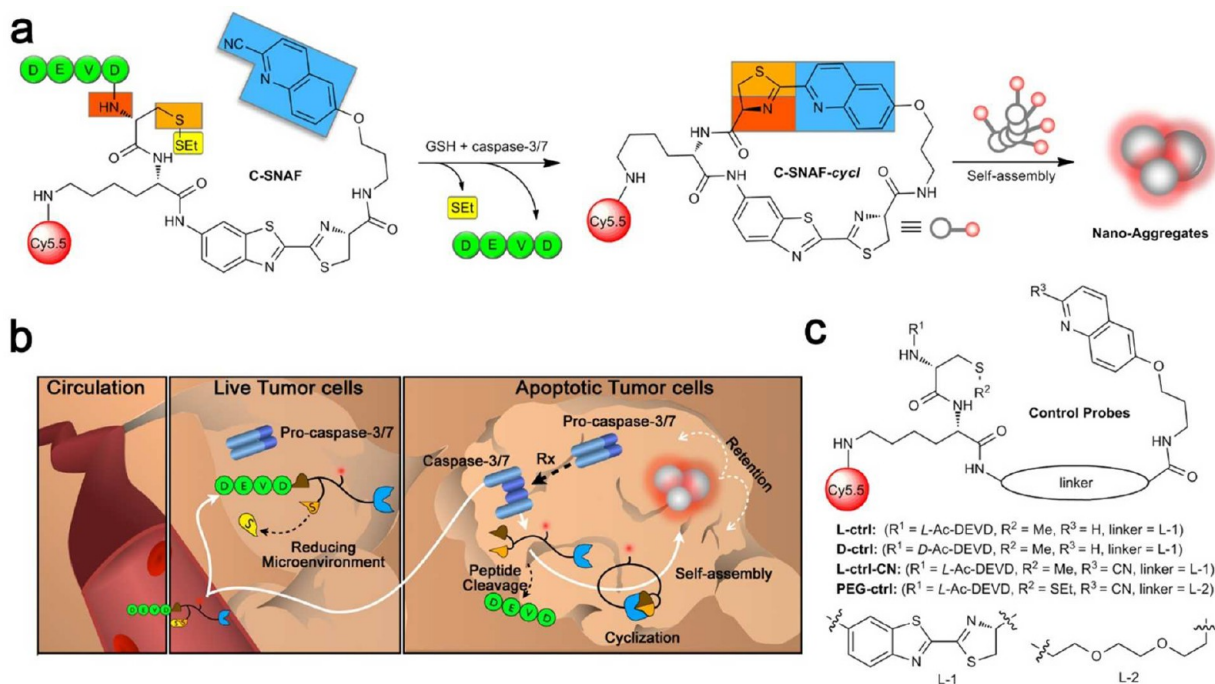


Figure 7. (A) Molecular design and the proposed conversion of C-SNAF into C-SNAF-cycl via reduction and caspase-3/7 activation of the biorthogonal intermolecular cyclization reaction, which is then followed by the self-assembly into nanoaggregates: green represents the capping peptide residues; dark orange, amino group of D-cysteine; light orange, thiol group of D-cysteine; yellow, thioethyl masking group, blue, the CHQ group; and red, the red NIR fluorophore Cy5.5. (B) Illustration of the mechanism of C-SNAF for *in vivo* imaging of tumor response following chemotherapy in living versus apoptotic cancer cells. (C) Chemical structures of probes used as controls for this study. Adapted with permission from ref 106. Copyright Nature Chemistry, 2014 Macmillan Publishers Ltd.

incorporates the same quencher, fluorophore, and CatB-degradable linker, but instead uses a GNNQQNY central assembly sequence derived from Sup35_{7–13} that can spontaneously associate into different morphologies based on temperature and incubation time in aqueous solutions. This sequence was modified with either three lysine or three glutamic acid residues for either positive or negative surface charge, and the probes were allowed to form either spherical or filamentous shapes. By observing cellular uptake by PC3-Flu metastatic human prostate cancer cells, they were able to show that positively charged nanobeacons had much higher uptake efficiency as opposed to its monomeric form, making this combination of shape and surface chemistry most-suited for intracellular sensing. The nanobeacon filaments had significantly lower internalization by cancer cells, making them more suitable for sensing extracellular proteases, like MMPs and uPA. The molecular design, nanobeacon characteristics, and confocal images and flow cytometry data of cellular uptake can be seen in Figure 6.¹⁰¹ Although *in vivo* work was not conducted, these studies are revealing of a nanoscale system with potential for significant tumor accumulation and accurate sensing based on the optimal shape and surface chemistry for their target protease.

Urokinase-Sensitive Systems. Urokinase-type plasminogen activator (uPA) of the urokinase-type plasminogen activator system is an attractive target for cancer sensitivity due to its overexpression in a handful of cancer lines and its presence on the exterior of the cell membrane. Over the past few years, molecular probes and nanomaterial systems responsive to uPA activity, particularly for breast cancer imaging, have been developed.¹⁰² For example, Law and co-workers developed a self-assembled nanofiber from a PEG₂₀₀₀-

peptide conjugate.¹⁰³ The uPA substrate, SGRSANA, served as a linker between the hydrophobic D-amino acid domain and the hydrophilic PEG domain with conjugated fluorescein isothiocyanate (FITC) for fluorescence imaging, where in the self-assembled state, no signal could be detected due to aggregation-induced quenching. Although only a proof-of-principle study, this group showed the applicability of their technology to *in vivo* uPA activity imaging for cancer detection.¹⁰³

Continuing with this concept, Law and co-workers developed an NIR molecular probe with a similar structure as mentioned before, with a PEG-based hydrophilic domain conjugated to the near-IR dye, NIR664, linked by a uPA-cleavable peptide sequence to a hydrophobic D-amino acid sequence, which allows for self-assembly into nanofibers in aqueous solution.¹⁰⁴ These nanofibers were able to detect uPA activity from several human cancer cell lines *in vitro* with very high fluorescence signals, giving more evidence to the applicability of these nanofibers for the diagnosis and even treatment of cancer based on different expression levels of uPA activity.¹⁰⁴

Another interesting nanomaterial design for cancer imaging via uPA proteolysis was developed by Stevens and co-workers.¹⁰⁵ They designed multiplex assay nanoparticles that are able to detect uPA activity and human epidermal growth factor receptor 2 (Her2) kinase activity, which are both overexpressed in breast cancer. Their system consists of two quantum dot (QD) populations with different emission wavelengths and orthogonal surface functionalizations for signal independence between the two different enzymes. The QDs serve not only as a reporter molecule but also as a scaffold for conjugates attached via enzyme-specific linker peptide sequences. The QD, QD525, was used for uPA-sensing and was

attached to the uPA-cleavable linker sequence, SGRSAN, which is covalently coupled to a gold nanoparticle that quenches the QD signal until cleaved away by uPA. A similar design was implemented for Her2 kinase detection, where phosphorylation of the Her2 kinase-sensitive linker induces FRET-based quenching. This system is the first demonstration of a nanoparticle-based activity assay being able to simultaneously sense the activity of two different classes of enzymes, which can provide prognostic information for breast cancer patients.¹⁰⁵

Caspase-Sensitive Systems. Caspases are useful imaging targets due to their role in programmed cell death, like apoptosis, and inflammation. The information obtained by visualizing when cells undergo apoptosis can elucidate information about the pharmacokinetics of a certain therapeutic and allow for long-term monitoring of drug response in a patient.⁸⁶ An example of a caspase-sensitive nanomaterial system is described here for visualization of cancer cell response to different chemotherapeutics.

A caspase-sensitive nanoaggregation fluorescent probe, called C-SNAF, was developed by Rao and co-workers that uses a biorthogonal cyclization reaction that triggers self-assembly and yields an aggregation-induced NIR fluorescence signal.¹⁰⁶ The C-SNAF probe contains D-cysteine and 2-cyano-6-hydroxyquinoline (CHQ) moieties that are linked to an amino luciferin scaffold. Additionally, it contains a L-DEVD capping sequence and a disulfide bond that are required for a two-step activation with caspase-3/7-mediated cleavage and an intracellular thiol-mediated reduction, which consequently promotes aggregation and gives NIR signal from Cy5.5 dye. Figure 7 details the molecular design of C-SNAF and the mechanism of nanoaggregation in live versus apoptotic tumor cells. As indicated by fluorescence and 3D-SIM imaging in Doxorubicin-treated mice tumor models, this probe is able to penetrate into tumor tissue after IV injection and successfully report tumor-cell death induced from chemotherapy *in vivo*. The probes are rigid and hydrophobic after undergoing cyclization that promotes nanoaggregation, where they are retained in apoptotic cells and give high imaging contrast for detection of therapeutic-response.¹⁰⁶

Rao and co-workers have expanded on this design to incorporate different imaging modalities. A Gd-based MRI probe, called C-SNAM, was developed, with prolonged accumulation in chemotherapy-induced apoptotic cells and tumors with significantly brighter contrast between treated and nontreated tumors.¹⁰⁷ Additionally, a ¹⁸F-based PET probe was developed which also had significantly higher tumor signal and tumor-to-muscle ratios in murine models in response to tumor therapy.^{108,109} The group also applied this technology for apoptosis imaging with caspase-activity in arthritis,¹¹⁰ highlighting the vast applicability of this probe design to imaging drug efficacy for many diseases.

■ PROTEASE-RESPONSIVE NANOMATERIAL SYSTEMS FOR THERANOSTICS

Many promising and efficacious systems have been developed for cancer imaging and drug delivery, which has helped sparked interest in studying and designing theranostic systems. These systems allow for simultaneous imaging and treatment and offer a means of visualizing the pharmacokinetics and biodistribution of therapeutics used for a cancer patient.²⁷ Theranostic nanomaterials can benefit from the incorporation of protease-sensitivity for improved selectivity, but multiresponsive systems that include protease-responsiveness have become popular for

designing more efficacious drug delivery and imaging systems. The nanomaterial systems can respond to other factors in the tumor microenvironment, such as cell-surface receptors,^{111,112} pH,^{73,113,114} and other classes of enzymes,¹¹⁵ thereby increasing sensitivity and selectivity and thus improving the overall efficacy of the cancer treatment. In this section, we will be discussing theranostic nanomaterial systems responsive to protease activity, including some examples that are sensitive to other factors in the tumor microenvironment.

An early example of the development of a theranostic probe was by Zheng and co-workers that showcased the possibility and advantages of simultaneous imaging and treatment of tumor cells.¹¹⁶ Their probe is capable of photodynamic therapy for cancer, where photodamage is induced via irradiation, and subsequently gives a near-infrared fluorescence signal to indicate successful induction of apoptosis. The molecular design contains the photosensitizing agent, purpophorbide *a* (Pyro), dual fluorescence and singlet oxygen quencher, BHQ-3, and a caspase-3-responsive peptide linker sequence, GDEVDGSGK. When tumor cells are irradiated with light in the presence of these molecular beacons, the photosensitizer converts oxygen into singlet oxygen, which destroys mitochondrial membranes and triggers apoptosis; therefore, caspase-3 expression will increase and act to cleave the linker sequence and give a detectable signal to indicate cell death. This design showed efficacy *in vitro* and was later shown to have *in vivo* efficacy after the incorporation of folate into the molecular design to target overexpressed folate receptors on the surfaces of cancer cells to induce endocytosis and improve selectivity to tumor tissue.^{116,117} Further work was done to improve design by instead using an MMP-7-sensitive linker for targeting to tumor cells, which simplified molecule complexity and synthesis requirements while also yielding comparable selectivity and therapeutic efficacy as earlier designs *in vitro* and *in vivo*.¹¹⁸ These beacons showcased mitigated nonspecific accumulation and enhanced tumor cell death in human breast carcinoma cells (MT-1 line) that commonly produce spinal metastases, where risks of spinal cord damage are very high, offering a safe approach of selective photodynamic therapy while preserving critical tissues.¹¹⁹ Their beacon design has shown efficacy for other types of cancer metastases without the incorporation of a nanomaterial, which could be useful in improving tumor accumulation, but regardless, the molecular beacons exemplify the utility of theranostics for cancer treatment.¹²⁰

Although the previously discussed example detailed an effective theranostic probe, using nanomaterials can prolong circulation time, reduce possibility of nonspecific activation, and increase accumulation at tumor sites.^{4,47} The laboratories of Kim and Ahn designed gold nanorods with MMP-sensitivity for cancer treatment and imaging.¹²¹ When irradiated, the gold nanorods absorb the near-infrared laser light and convert it into heat as a means of hyperthermal therapy for cancer cells, which are more susceptible to treatment due to their lower heat tolerance from poor blood supply. The near-infrared dye Cy5.5 was conjugated to the surface of the nanorods via the MMP-sensitive peptide linker sequence, GPLGVRGC, which is responsive to a variety of MMPs. Gold is a popular material for imaging due to its exhibition of surface plasmon resonance, where it can serve as a fluorescence quencher as it does in this design. These nanorods were studied with HeLa cells *in vitro* and with SCC-7 tumors in mice, where the nanorods showed the ability to kill cancer cells effectively and very rapidly, as temperatures could increase over 45 °C in little as 4 min.

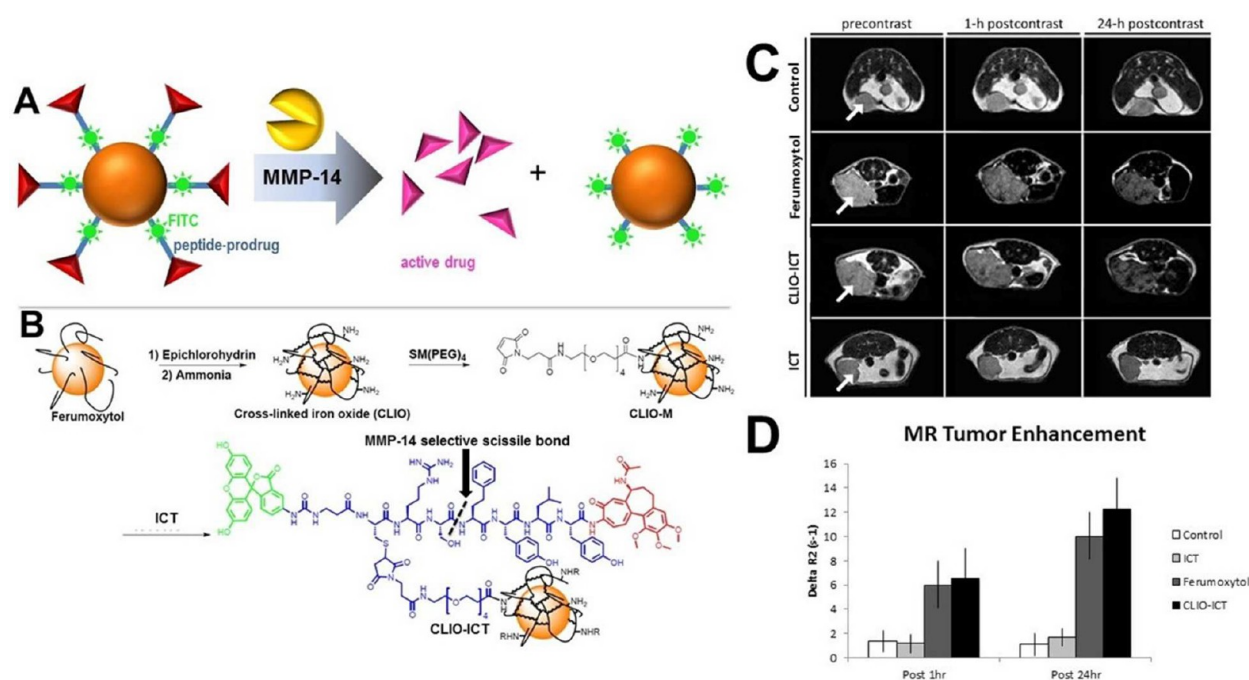


Figure 8. (A) Schematic illustration representing the activation of the theranostic nanoparticles, CLIO-ICT, by MMP-14 cleavage. The iron oxide nanoparticle (IONP) is shown in orange; the prodrug azademethylcolchicine (ICT) is shown in red, and its product after MMP-14 degradation is shown in magenta; the MMP-14 sensitive peptide linker is shown in blue; and the green fluorophore, fluorescein isothiocyanate (FITC), is shown in green. (B) Synthesis pathway for the CLIO-ICT theranostic nanoparticles, highlighting cross-linking and ICT prodrug addition. (C) Axial T_2 -weighted MR images of MMTV-PyMT mammary tumors before and after a single IV injection of either 0.6 M (Fe) solution of ferumoxytol, 0.4 M solution of CLIO-ICT, 0.29 mM solution of ICT, or PBS, where contrast agent accumulation is indicated as a negative (dark) signal enhancement of the tumors. (D) Corresponding MR signal enhancement data of tumors in panel C quantified as $\Delta R_2 = (R_{2\text{pre}} - R_{2\text{post}})$. Adapted with permission from ref 124. Copyright 2014 John Wiley and Sons.

However, the external skin of the mice was burned at tumor sites and nonspecific damage seems unavoidable with this design. Only the imaging function of this design is sensitive to the overexpressed MMP activity in tumors and the therapeutic function can be delivered regardless of MMP presence; therefore, further modifications could be added for improving selectivity. However, this does represent a unique therapeutic approach, and it showcases the importance of selectivity and the utility that gold possesses for theranostic applications.¹²¹

In another example of utilizing inorganic nanostructures, Cheng and Xing report the design of a protease-responsive, core-shell, dual-imaging magnetic silica-coated nanoparticles.¹²² The anticancer-drug, doxorubicin (Dox), is conjugated to a cathepsin B-cleavable peptide sequence (FK) with a *para*-aminobenzyloxycarbonyl (PABC) linker, and through click chemistry, they are attached to the surface of uniform silica-coated, superparamagnetic iron oxide nanoparticles via an azido-dPEG₄ linker. Doxorubicin is a red fluorescent drug, which in conjunction with the iron oxide nanoparticles, allows for dual-modality imaging of both MRI and optical imaging. With confocal microscopy and MRI spectroscopy, they showed highly efficient release of Dox upon interaction with cathepsin B in HT-29 cancer cells *in vitro*. Cell viability was comparable between nanoparticle-treated and free drug-treated cells but was much higher for the nanoparticle-treated negative control cells than free drug, indicating that the nanoparticles function to give selective tumor intracellular drug delivery and imaging while keeping healthy tissues safe.¹²² This system, while showcasing dual-modality for imaging, also contains an intrinsically theranostic moiety in Dox, which greatly improves efficacy as a theranostic for cancer.

Expanding upon this notion of intrinsically theranostic systems, by using moieties capable of both imaging and therapy in the design of nanomaterial systems for cancer, there is no longer a need to compromise on the extent of loading between imaging and therapeutic moieties nor long lag time periods present between drug activation and corresponding optical signal. Cui and co-workers developed, to the best of their knowledge, the first enzyme-specific Dox prodrug conjugated with a dark chromophore quencher capable of both diagnostic and therapeutic functions.¹²³ Their FRET-based molecular probe contains red-fluorescent anticancer drug, Dox, a black hole quencher (BHQ-2) conjugated via a cathepsin B-sensitive peptide linker (GFLG), and a cell-penetrating peptide sequence (R8) to help circumvent drug resistance in some cancer lines. Confocal images taken of NCI/ADR-Res ovarian cancer cells, which are resistant to Dox, indicate the efficacy of the drug-beacons to simultaneously image and treat cancer while overcoming drug resistance, as the drug-beacons showed significantly better cytotoxicity in comparison to free Dox. Although this system does not incorporate any nanomaterials, the beacons could be modified to self-assemble into nanostructures for *in vivo* efficacy. The intrinsic theranostic ability of this system simplifies molecular design and offers sufficient drug loading with direct visualization of drug activation.¹²³

In another example, Rao and Daldrup-Link report the design of a novel, multifunctional theranostic nanoparticle with the capability to release drugs via enzymatic cleavage and to give MR and fluorescence imaging of drug delivery *in vivo*.¹²⁴ The design incorporates a magnetic iron oxide nanoparticle, ferumoxytol, conjugated to an MMP-14-responsive peptide

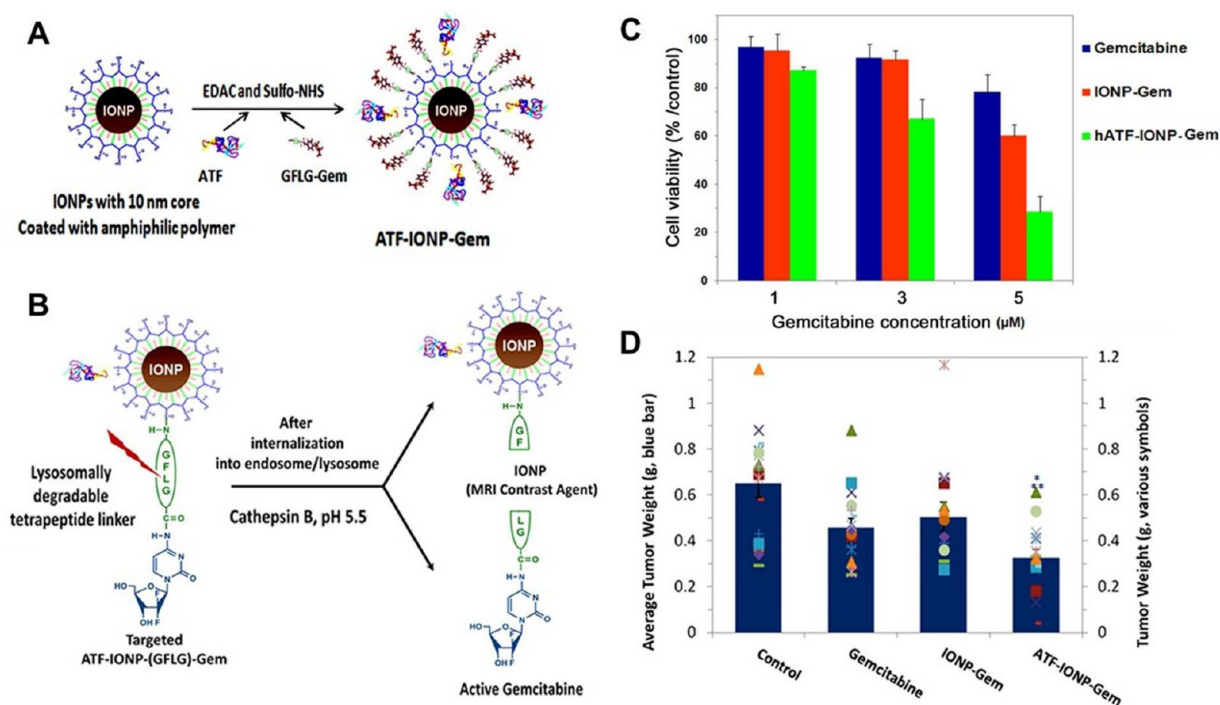


Figure 9. (A) Illustration of the conjugation of the amino-terminal fragment peptides of the receptor-binding domain of uPA (ATF), the cathepsin B-sensitive linker, and anticancer drug gemcitabine (GFLG-Gem) conjugates to the surface of iron oxide nanoparticles (IONPs), forming ATF-IONP-Gem. (B) Schematic representation of the release of gemcitabine after cathepsin B-cleavage from ATF-IONP-Gem. (C) Data from a cell proliferation assay conducted on MIA PaCa-2 cells after 4 h treatment with free Gem, IONP-Gem, or ATF-IONP-Gem followed by 72 h incubation, indicating high reduction in cell viability from conjugation of Gem to IONPs with targeting for uPAR and cathepsin B. (D) Further evidence of improved efficacy of ATF-IONP-Gem from tumor xenograft mice models by comparing mean tumor weights and individual tumor weight distributions of mice in each group represented by colored symbols. Adapted with permission from ref 125. Copyright 2013 American Chemical Society.

sequence that holds the green-fluorescent dye, fluorescein isothiocyanate (FITC), and a vascular disrupting agent, azademethylcolchicine (ICT), creating a theranostic probe they call CLIO-ICTs. The molecular design and mechanism of action of CLIO-ICTs are detailed in Figure 8. Upon treatment of MMP-14-positive MMTV-PyMT breast cancer cells with CLIO-ICTs, significant cell death was observed *in vitro*, but not for cells treated with ferumoxytol alone nor MMP-14-negative fibroblasts, indicating MMP-14-sensitivity is needed for effective delivery. Tumor-bearing mice were given IV injections of the nanoparticles, and subsequent MR imaging showed significant tumor accumulation of CLIO-ICT and was confirmed with histopathology staining, further demonstrating the selectivity of the nanoparticles to tumors and not healthy tissues. MR images and corresponding signal data are given in Figure 8. The dual-modality imaging offers the advantages of both techniques in a single probe that also treats cancer, the nanostructure design increases tumor retention, and together, improve the overall antitumor efficacy.¹²⁴

Although protease-responsiveness is an effective means of increasing tumor selectivity, incorporating other factors of the tumor microenvironment alongside protease-activation can further improve cancer targeting. The groups of Mao and Yang report on the design and effectiveness of urokinase plasminogen activator receptor (uPAR)-targeted, cathepsin B-sensitive magnetic iron oxide nanoparticles (IONPs) that carry the chemotherapeutic drug gemcitabine (Gem).¹²⁵ The iron oxide nanoparticles are conjugated with an amino-terminal fragment peptide (ATF) of the receptor-binding domain of uPA and Gem via a cathepsin B-cleavable peptide linker

(GFLG) on their surfaces, with nanoparticles being called ATF-IONP-Gem. The molecular design specifics and means of activation are detailed in Figure 9. The nanoparticles showed higher drug release in more acidic surroundings, which is representative of the lysosomal and endosomal environments that contain cathepsins. *In vitro* and *in vivo* studies of ATF-IONP-Gem efficacy with the MIA PaCa-2 human pancreatic cancer cell line showed that free Gem only inhibited tumor growth by 30%, whereas ATF-IONP-Gem exhibited approximately 50% tumor growth inhibition in xenograft mice. Cell viability and tumor weight data post-treatment are provided in Figure 9. The delivery of ATF-IONP-Gem and presence of residual tumors could then be detected noninvasively by MRI using both T₂-weighted and T₁-weighted ultrasound echo time imaging, allowing for monitoring and assessment of treatment efficacy. The significant difference in tumor treatment between nanoparticles with only cathepsin B-sensitivity and those with uPAR and cathepsin B-targeting emphasizes the increasing selectivity to tumor tissue by incorporating responsiveness to multiple factors in the tumor microenvironment, which is promising for the development of safer and more personalized medicine in the future via theranostics.¹²⁵

CONCLUSION

A better understanding of the molecular basis of many diseases has been developed over the years, particularly in regards to cancer, leading to the identification of microenvironment factors and cellular features that are representative of diseased tissues. These factors have been significantly beneficial in

improving the efficacy and selectivity of imaging agents and therapeutics to tumor tissues. Proteases, which are overexpressed in many cancer types at various cellular locations, play important roles in cancer progression, and therefore represent attractive targets for diagnostics and therapeutics. Nanotechnology can further improve the efficacy of imaging agents and pharmaceuticals, where design factors can be modified to influence the characteristics of nanomaterials and impact their delivery properties, primarily through improvement of the pharmacokinetic profile and biodistribution of molecular probes and free drugs. The combination of imaging and therapeutics has opened a new field of medicine called theranostics, producing systems that possess the ability to monitor drug delivery, drug release, and drug efficacy using a single entity. Incorporating protease-responsiveness into a theranostic platform can assist with early stage cancer diagnosis, give an accurate evaluation of cancer progression, and noninvasively provide real time information to healthcare providers to choose appropriate medical treatments. Such multifunctional platforms can improve clinical outcomes and pave the way toward personalized medicine. In this review, we have discussed recent examples of therapeutic, diagnostic, and theranostic nanomaterial systems that have proven useful for cancer treatment.

Looking forward, the selection of the proper protease target is critical in theranostic system design, as some proteases may prove more beneficial for imaging or drug delivery based on their location in, on, or around cancer cells. Signals and delivery are susceptible to protease location, quantity, and activity, which can vary and are not uniform among all cancer types. Multiple modalities for imaging can give the benefits of multiple techniques in a single probe, yielding more information, but this can complicate the manufacturing process and reproducibility of signals. Although targeting multiple environmental factors increases selectivity, finding the optimal combination to maximize selectivity and preserve healthy tissues is necessary. Additionally, the sequence in which the system will respond to these factors must be considered for the highest efficacy. Trade-offs occur when combining imaging and therapy, such as compromising on the loading of one agent over the other, accounting for the difference in the necessary concentration for good imaging contrast and therapeutic response, and considering the optimal circulation times between different agents (imaging agents benefit from faster clearance whereas therapeutics benefit from sustained delivery). These issues can be addressed by using molecules that possess both imaging and therapeutic properties and work should be done to develop these types of theranostic probes. Addressing these challenges will yield better clinical outcomes for cancer treatment and bring us closer to personalized medicine.

■ AUTHOR INFORMATION

Corresponding Author

*Honggang Cui, email: hcui6@jhu.edu.

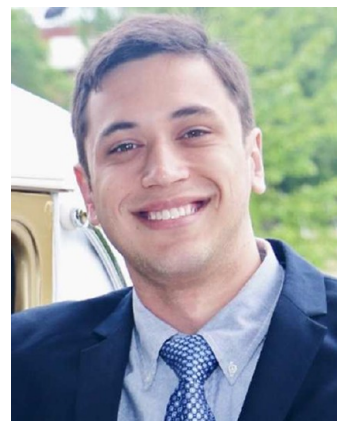
ORCID

Honggang Cui: 0000-0002-4684-2655

Notes

The authors declare no competing financial interest.

Biographies



Caleb F. Anderson received a Bachelor's degree in Chemical and Biomolecular Engineering from the Georgia Institute of Technology in 2016. He is currently a Ph.D. student in Dr. Honggang Cui's laboratory in the department of Chemical and Biomolecular Engineering at the Johns Hopkins University. His research interests include theranostics, peptide-based nanomaterials, and drug development and delivery systems.



Honggang Cui received a Bachelor's degree in Polymer Materials Science and Engineering from the Beijing University of Chemical Technology in 1999, a Master's degree in Materialogy/Chemical Engineering from Tsinghua University in 2002, and a Ph.D. degree in Materials Science and Engineering from the University of Delaware in 2007. He was a postdoctoral fellow between 2007 and 2010 in the department of Materials Science and Engineering and the Institute for BioNanotechnology in Medicine at Northwestern University. He joined the Chemical and Biomolecular Engineering department at the Johns Hopkins University as assistant professor in 2010, and also holds joint appointments in the Department of Oncology and Sidney Kimmel Comprehensive Cancer Center, and the Center for Nanomedicine of Wilmer Eye Institute at the Johns Hopkins University School of Medicine. He is a recipient of the NSF CAREER Award, the 3M Non-Tenured Faculty Award, the Johns Hopkins Catalysis Award. His research focuses on the design, synthesis and functional assembly of peptidic molecules and therapeutic agents for applications in drug delivery, cancer diagnosis and imaging, and tumor microenvironment mimicking.

■ ACKNOWLEDGMENTS

This invited contribution is part of the I&EC Research special issue for the 2017 Class of Influential Researchers. This work was supported by the National Science Foundation (DMR 1255281) and the National Institutes of Health (NIH/

R21CA191740). We also thank Daryl Anderson for his contribution in the development of our illustrations.

REFERENCES

- (1) Torchilin, V. P. Multifunctional, Stimuli-Sensitive Nanoparticle Systems for Drug Delivery. *Nat. Rev. Drug Discovery* **2014**, *13*, 813–827.
- (2) Keliher, E. J.; Reiner, T.; Earley, S.; Klubnick, J.; Tassa, C.; Lee, A. J.; Ramaswamy, S.; Bardeesy, N.; Hanahan, D.; Depinho, R. A.; Castro, C. M.; Weissleder, R. Targeting Cathepsin E in Pancreatic Cancer by a Small Molecule Allows In Vivo Detection. *Neoplasia* **2013**, *15*, 684–693.
- (3) De La Rica, R.; Aili, D.; Stevens, M. M. Enzyme-Responsive Nanoparticles for Drug Release and Diagnostics. *Adv. Drug Delivery Rev.* **2012**, *64*, 967–978.
- (4) Hu, Q.; Katti, P. S.; Gu, Z. Enzyme-Responsive Nanomaterials for Controlled Drug Delivery. *Nanoscale* **2014**, *6*, 12273–12286.
- (5) Sun, X.; Li, Y.; Liu, T.; Li, Z.; Zhang, X.; Chen, X. Peptide-Based Imaging Agents for Cancer Detection. *Adv. Drug Delivery Rev.* **2016**, DOI: 10.1016/j.addr.2016.06.007.
- (6) Liu, T. W. B.; Chen, J.; Zheng, G. Peptide-Based Molecular Beacons for Cancer Imaging and Therapy. *Amino Acids* **2011**, *41*, 1123–113.
- (7) Duffy, M. J. The Role of Proteolytic Enzymes in Cancer Invasion and Metastasis. *Clin. Exp. Metastasis* **1992**, *10*, 145–155.
- (8) Chen, S.; Cui, J.; Jiang, T.; Olson, E. S.; Cai, Q.-Y.; Yang, M.; Wu, W.; Guthrie, J. M.; Robertson, J.; Lipton, S. A.; Ma, L.; Tsien, R. Y.; Gu, Z. Gelatinase Activity Imaged by Activatable Cell-Penetrating Peptides in Cell-Based and in Vivo Models of Stroke. *J. Cereb. Blood Flow Metab.* **2015**, *37*, 1–13.
- (9) Nejadnik, H.; Ye, D.; Lenkov, O. D.; Donig, J. S.; Martin, J. E.; Castillo, R.; Derugin, N.; Sennino, B.; Rao, J.; Daldrup-Link, H. Magnetic Resonance Imaging of Stem Cell Apoptosis in Arthritic Joints with a Caspase Activatable Contrast Agent. *ACS Nano* **2015**, *9*, 1150–1160.
- (10) Maeda, H. The Enhanced Permeability and Retention (EPR) Effect in Tumor Vasculature: The Key Role of Tumor-Selective Macromolecular Drug Targeting. *Adv. Enzyme Regul.* **2001**, *41*, 189–207.
- (11) Wang, Y.; Zhou, K.; Huang, G.; Hensley, C.; Huang, X.; Ma, X.; Zhao, T.; Sumer, B. D.; Deberardinis, R. J.; Gao, J. A Nanoparticle-Based Strategy for the Imaging of a Broad Range of Tumours by Nonlinear Amplification of Microenvironment Signals. *Nat. Mater.* **2014**, *13*, 204–212.
- (12) Lee, H.; Akers, W.; Bhushan, K.; Bloch, S.; Sudlow, G.; Tang, R.; Achilefu, S. Near-Infrared pH-Activatable Fluorescent Probes for Imaging Primary and Metastatic Breast Tumors. *Bioconjugate Chem.* **2011**, *22*, 777–784.
- (13) Ji, T.; Zhao, Y.; Wang, J.; Zheng, X.; Tian, Y.; Zhao, Y.; Nie, G. Tumor Fibroblast Specific Activation of a Hybrid Ferritin Nanocage-Based Optical Probe for Tumor Microenvironment Imaging. *Small* **2013**, *9*, 2427–2431.
- (14) Wang, Y.; Cheetham, A. G.; Angacian, G.; Su, H.; Xie, L.; Cui, H. Peptide–drug Conjugates as Effective Prodrug Strategies for Targeted Delivery. *Adv. Drug Delivery Rev.* **2016**, DOI: 10.1016/j.addr.2016.06.015.
- (15) Cheetham, A. G.; Zhang, P.; Lin, Y.-A.; Lock, L. L.; Cui, H. Supramolecular Nanostructures Formed by Anticancer Drug Assembly. *J. Am. Chem. Soc.* **2013**, *135*, 2907–2910.
- (16) Chen, B.; Dai, W.; He, B.; Zhang, H.; Wang, X.; Wang, Y.; Zhang, Q. Current Multistage Drug Delivery Systems Based on the Tumor Microenvironment. *Theranostics* **2017**, *7*, 538–558.
- (17) Lu, Y.; Sun, W.; Gu, Z. Stimuli-Responsive Nanomaterials for Therapeutic Protein Delivery. *J. Controlled Release* **2014**, *194*, 1–19.
- (18) Mura, S.; Nicolas, J.; Couvreur, P. Stimuli-Responsive Nanocarriers for Drug Delivery. *Nat. Mater.* **2013**, *12*, 991–1003.
- (19) Young Choi, K.; Swierczewska, M.; Lee, S.; Chen, X. Protease-Activated Drug Development. *Theranostics* **2012**, *2*, 156–178.
- (20) Bremer, C.; Tung, C.-H.; Bogdanov, A.; Weissleder, R. Imaging of Differential Protease Expression in Breast Cancers for Detection of Aggressive Tumor Phenotypes. *Radiology* **2002**, *222*, 814–818.
- (21) Huang, P.; Gao, Y.; Lin, J.; Hu, H.; Liao, H.-S.; Yan, X.; Tang, Y.; Jin, A.; Song, J.; Niu, G.; Zhang, G.; Horkay, F.; Chen, X. Tumor-Specific Formation of Enzyme-Instructed Supramolecular Self-Assemblies as Cancer Theranostics. *ACS Nano* **2015**, *9*, 9517–9527.
- (22) Blum, G.; Von Degenfeld, G.; Merchant, M. J.; Blau, H. M.; Bogoy, M. Noninvasive Optical Imaging of Cysteine Protease Activity Using Fluorescently Quenched Activity-Based Probes. *Nat. Chem. Biol.* **2007**, *3*, 668–677.
- (23) Joyce, J. A.; Baruch, A.; Chehade, K.; Meyer-Morse, N.; Giraudo, E.; Tsai, F.-Y.; Greenbaum, D. C.; Hager, J. H.; Bogoy, M.; Hanahan, D. Cathepsin Cysteine Proteases Are Effectors of Invasive Growth and Angiogenesis during Multistage Tumorigenesis. *Cancer Cell* **2004**, *5*, 443–453.
- (24) Gialeli, C.; Theocharis, A. D.; Karamanos, N. K. Roles of Matrix Metalloproteinases in Cancer Progression and Their Pharmacological Targeting. *FEBS J.* **2011**, *278*, 16–27.
- (25) Vartak, D. G.; Gemeinhart, R. A. Matrix Metalloproteinases: Underutilized Targets for Drug Delivery. *J. Drug Target.* **2007**, *15*, 1–20.
- (26) Lopez-Otin, C.; Matrisian, L. M. Emerging Roles of Proteases in Tumour Suppression. *Nat. Rev. Cancer* **2007**, *7*, 800–808.
- (27) Ahmed, N.; Fessi, H.; Elaissari, A. Theranostic Applications of Nanoparticles in Cancer. *Drug Discovery Today* **2012**, *17*, 928–934.
- (28) Kelkar, S. S.; Reineke, T. M. Theranostics: Combining Imaging and Therapy. *Bioconjugate Chem.* **2011**, *22*, 1879–1903.
- (29) Torchilin, V. P. Recent Advances with Liposomes as Pharmaceutical Carriers. *Nat. Rev. Drug Discovery* **2005**, *4*, 145–160.
- (30) Baker, J. R. Dendrimer-Based Nanoparticles for Cancer Therapy. *Hematology* **2009**, *14*, 708–719.
- (31) Chen, W.; Ayala-Orozco, C.; Biswal, N. C.; Perez-Torres, C.; Bartels, M.; Bardhan, R.; Stinnet, G.; Liu, X.-D.; Ji, B.; Deorukhkar, A.; Brown, L. V.; Guha, S.; Pautler, R. G.; Krishnan, S.; Halas, N. J.; Joshi, A. Targeting of Pancreatic Cancer with Magneto-Fluorescent Theranostic Gold Nanoshells. *Nanomedicine (London, U. K.)* **2014**, *9*, 1209–1222.
- (32) Rosi, N. L.; Mirkin, C. A. Nanostructures in Biodiagnostics. *Chem. Rev.* **2005**, *105*, 1547–1562.
- (33) Sun, T.; Zhang, Y. S.; Pang, B.; Hyun, D. C.; Yang, M.; Xia, Y. Engineered Nanoparticles for Drug Delivery in Cancer Therapy. *Angew. Chemie - Int. Ed.* **2014**, *53*, 12320–12364.
- (34) Kuang, Y.; Shi, J.; Li, J.; Yuan, D.; Alberti, K. A.; Xu, Q.; Xu, B. Pericellular Hydrogel/nanonets Inhibit Cancer Cells. *Angew. Chem., Int. Ed.* **2014**, *53*, 8104–8107.
- (35) Zhao, F.; Lung Ma, M.; Xu, B. Molecular Hydrogels of Therapeutic Agents. *Chem. Soc. Rev.* **2009**, *38*, 883–891.
- (36) Chau, Y.; Luo, Y.; Cheung, A. C. Y.; Nagai, Y.; Zhang, S.; Kobler, J. B.; Zeitels, S. M.; Langer, R. Incorporation of a Matrix Metalloproteinase-Sensitive Substrate into Self-Assembling Peptides - A Model for Biofunctional Scaffolds. *Biomaterials* **2008**, *29*, 1713–1719.
- (37) Carter, P. J.; Senter, P. D. Antibody-Drug Conjugates for Cancer Therapy. *Cancer J.* **2008**, *14*, 154–169.
- (38) Zhang, L.; Chan, J. M.; Gu, F. X.; Rhee, J. W.; Wang, A. Z.; Radovic-Moreno, A. F.; Alexis, F.; Langer, R.; Farokhzad, O. C. Self-Assembled Lipid-Polymer Hybrid Nanoparticles: A Robust Drug Delivery Platform. *ACS Nano* **2008**, *2*, 1696–1702.
- (39) Cheng, J.; Tepley, B. A.; Sherif, I.; Sung, J.; Luther, G.; Gu, F. X.; Levy-Nissenbaum, E.; Radovic-Moreno, A. F.; Langer, R.; Farokhzad, O. C. Formulation of Functionalized PLGA-PEG Nanoparticles for in Vivo Targeted Drug Delivery. *Biomaterials* **2007**, *28*, 869–876.
- (40) Peer, D.; Karp, J. M.; Hong, S.; Farokhzad, O. C.; Margalit, R.; Langer, R. Nanocarriers as an Emerging Platform for Cancer Therapy. *Nat. Nanotechnol.* **2007**, *2*, 751–760.
- (41) Choi, H. S.; Liu, W.; Liu, F.; Nasr, K.; Misra, P.; Bawendi, M. G.; Frangioni, J. V. Design Considerations for Tumour-Targeted Nanoparticles. *Nat. Nanotechnol.* **2010**, *5*, 42–47.

- (42) Lee, D.-E.; Koo, H.; Sun, I.-C.; Hee Ryu, J.; Kim, K.; Chan Kwon, I. Multifunctional Nanoparticles for Multimodal Imaging and Theragnosis. *Chem. Soc. Rev.* **2012**, *41*, 2656–2672.
- (43) Geng, Y.; Dalhaimer, P.; Cai, S.; Tsai, R.; Tewari, M.; Minko, T.; Discher, D. E. Shape Effects of Filaments versus Spherical Particles in Flow and Drug Delivery. *Nat. Nanotechnol.* **2007**, *2*, 249–255.
- (44) Ma, W.; Cheetham, A. G.; Cui, H. Building Nanostructures with Drugs. *Nano Today* **2015**, *11*, 13–30.
- (45) Wagh, A.; Singh, J.; Qian, S.; Law, B. A Short Circulating Peptide Nanofiber as a Carrier for Tumoral Delivery. *Nanomedicine* **2013**, *9*, 449–457.
- (46) Yu, M. K.; Park, J.; Jon, S.; Sangyong, J. Targeting Strategies for Multifunctional Nanoparticles in Cancer Imaging and Therapy. *Theranostics* **2012**, *2*, 3–44.
- (47) Su, H.; Koo, J. M.; Cui, H. One-Component Nanomedicine. *J. Controlled Release* **2015**, *219*, 383–395.
- (48) Gao, Y.; Shi, J.; Yuan, D.; Xu, B. Imaging Enzyme-Triggered Self-Assembly of Small Molecules inside Live Cells. *Nat. Commun.* **2012**, *1*, 1033–1038.
- (49) Razgulín, A.; Ma, N.; Rao, J. Strategies for in Vivo Imaging of Enzyme Activity: An Overview and Recent Advances. *Chem. Soc. Rev.* **2011**, *40*, 4186–4216.
- (50) Cai, Y.; Shi, Y.; Wang, H.; Wang, J.; Ding, D.; Wang, L.; Yang, Z. Environment-Sensitive Fluorescent Supramolecular Nanofibers for Imaging Applications. *Anal. Chem.* **2014**, *86*, 2193–2199.
- (51) Tung, C.; Mahmood, U.; Bredow, S.; Weissleder, R. In Vivo Imaging of Proteolytic Enzyme Activity Using a Novel Molecular Reporter In Vivo Imaging of Proteolytic Enzyme Activity Using a Novel Molecular Reporter I. *Cancer Res.* **2000**, *60*, 4953–4958.
- (52) Weissleder, R.; Tung, C.-H.; Mahmood, U.; Bogdanov, A. In Vivo Imaging of Tumors with Protease-Activated near-Infrared Fluorescent Probes. *Nat. Biotechnol.* **1999**, *17*, 375–378.
- (53) Weissleder, R.; Pittet, M. J. Imaging in the Era of Molecular Oncology. *Nature* **2008**, *452*, 580–589.
- (54) Willmann, J. K.; van Bruggen, N.; Dinkelborg, L. M.; Gambhir, S. S. Molecular Imaging in Drug Development. *Nat. Rev. Drug Discovery* **2008**, *7*, 591–607.
- (55) Zhang, P.; Cheetham, A. G.; Lock, L. L.; Li, Y.; Cui, H. Activatable Nanoprobes for Biomolecular Detection. *Curr. Opin. Biotechnol.* **2015**, *34*, 171–179.
- (56) Liu, S.; Zhang, P.; Banerjee, S. R.; Xu, J.; Pomper, M. G.; Cui, H. Design and Assembly of Supramolecular Dual-Modality Nanoprobes. *Nanoscale* **2015**, *7*, 9462–9466.
- (57) Ryu, J. H.; Koo, H.; Sun, I.-C.; Yuk, S. H.; Choi, K.; Kim, K.; Kwon, I. C. Tumor-Targeting Multi-Functional Nanoparticles for Theragnosis: New Paradigm for Cancer Therapy. *Adv. Drug Delivery Rev.* **2012**, *64*, 1447–1458.
- (58) Cheng, Z.; Al Zaki, A.; Hui, J. Z.; Muzykantov, V. R.; Tsourkas, A. Multifunctional Nanoparticles: Cost Versus Benefit of Adding Targeting and Imaging Capabilities. *Science* **2012**, *338*, 903–910.
- (59) Janib, S. M.; Moses, A. S.; Mackay, J. A. Imaging and Drug Delivery Using Theranostic Nanoparticles. *Adv. Drug Delivery Rev.* **2010**, *62*, 1052–1063.
- (60) Lammers, T.; Aime, S.; Hennink, W. E.; Storm, G.; Kiessling, F. Theranostic Nanomedicine. *Acc. Chem. Res.* **2011**, *44*, 1029–1038.
- (61) Terreno, E.; Uggeri, F.; Aime, S. Image Guided Therapy: The Advent of Theranostic Agents. *J. Controlled Release* **2012**, *161*, 328–337.
- (62) Mura, S.; Couvreur, P. Nanotheranostics for Personalized Medicine. *Adv. Drug Delivery Rev.* **2012**, *64*, 1394–1416.
- (63) Jiang, T.; Mo, R.; Bellotti, A.; Zhou, J.; Gu, Z. Gel-Liposome-Mediated Co-Delivery of Anticancer Membrane-Associated Proteins and Small-Molecule Drugs for Enhanced Therapeutic Efficacy. *Adv. Funct. Mater.* **2014**, *24*, 2295–2304.
- (64) Langer, R.; Weissleder, R. Nanotechnology. *JAMA* **2015**, *313*, 135–136.
- (65) Li, S.-D.; Huang, L. Pharmacokinetics and Biodistribution of Nanoparticles. *Mol. Pharmaceutics* **2008**, *5*, 496–504.
- (66) Albright, C. F.; Graciani, N.; Han, W.; Yue, E.; Stein, R.; Lai, Z.; Diamond, M.; Dowling, R.; Grimminger, L.; Zhang, S.-Y.; Behrens, D.; Musselman, A.; Bruckner, R.; Zhang, M.; Jiang, X.; Hu, D.; Higley, A.; Dimeo, S.; Rafalski, M.; Mandlekar, S.; Car, B.; Yeleswaram, S.; Stern, A.; Copeland, R. A.; Combs, A.; Seitz, S. P.; Trainor, G. L.; Taub, R.; Huang, P.; Oliff, A. Matrix Metalloproteinase-Activated Doxorubicin Prodrugs Inhibit HT1080 Xenograft Growth Better than Doxorubicin with Less Toxicity. *Mol. Cancer Ther.* **2005**, *4*, 751–760.
- (67) Chen, Z.; Zhang, P.; Cheetham, A. G.; Moon, J. H.; Moxley, J. W.; Lin, Y.-A.; Cui, H. Controlled Release of Free Doxorubicin from Peptide–drug Conjugates by Drug Loading. *J. Controlled Release* **2014**, *191*, 123–130.
- (68) Veiman, K.-L.; Künnapuu, K.; Lehto, T.; Kiisholts, K.; Pärn, K.; Langel, Ü.; Kurrikoff, K. PEG Shielded MMP Sensitive CPPs for Efficient and Tumor Specific Gene Delivery in Vivo. *J. Controlled Release* **2015**, *209*, 238–247.
- (69) Zhu, L.; Wang, T.; Perche, F.; Taigind, A.; Torchilin, V. P. Enhanced Anticancer Activity of Nanopreparation Containing an MMP2-Sensitive PEG-Drug Conjugate and Cell-Penetrating Moiety. *Proc. Natl. Acad. Sci. U. S. A.* **2013**, *110*, 17047–17052.
- (70) Andreasen, P. A.; Kjoller, L.; Christensen, L.; Duffy, M. J. The Urokinasectype Plasminogen Activator System in Cancer Metastasis. *Int. J. Cancer* **1997**, *72*, 1–22.
- (71) Basel, M. T.; Shrestha, T. B.; Troyer, D. L.; Bossmann, S. H. Protease-Sensitive, Polymer-Caged Liposomes: A Method for Making Highly Targeted Liposomes Using Triggered Release. *ACS Nano* **2011**, *5*, 2162–2175.
- (72) Cheng, Y.-J.; Luo, G.-F.; Zhu, J.-Y.; Xu, X.-D.; Zeng, X.; Cheng, D.-B.; Li, Y.-M.; Wu, Y.; Zhang, X.-Z.; Zhuo, R.-X.; He, F. Enzyme-Induced and Tumor-Targeted Drug Delivery System Based on Multifunctional Mesoporous Silica Nanoparticles. *ACS Appl. Mater. Interfaces* **2015**, *7*, 9078–9087.
- (73) Huang, S.; Shao, K.; Kuang, Y.; Liu, Y.; Li, J.; An, S.; Guo, Y.; Ma, H.; He, X.; Jiang, C. Tumor Targeting and Microenvironment-Responsive Nanoparticles for Gene Delivery. *Biomaterials* **2013**, *34*, 5294–5302.
- (74) Kulkarni, P. S.; Haldar, M. K.; Nahire, R. R.; Katti, P.; Ambre, A. H.; Muhonen, W. W.; Shabb, J. B.; Padi, S. K. R.; Singh, R. K.; Borowicz, P. P.; Shrivastava, D. K.; Katti, K. S.; Reindl, K.; Guo, B.; Mallik, S. MMP-9 Responsive PEG Cleavable Nanovesicles for Efficient Delivery of Chemotherapeutics to Pancreatic Cancer. *Mol. Pharmaceutics* **2014**, *11*, 2390–2399.
- (75) Tanaka, A.; Fukuoka, Y.; Morimoto, Y.; Honjo, T.; Koda, D.; Goto, M.; Maruyama, T. Cancer Cell Death Induced by the Intracellular Self-Assembly of an Enzyme-Responsive Supramolecular Gelator. *J. Am. Chem. Soc.* **2015**, *137*, 770–775.
- (76) Yang, B. Z.; Gu, H.; Fu, D.; Gao, P.; Lam, J. K.; Xu, B. Enzymatic Formation of Supramolecular Hydrogels. *Adv. Mater.* **2004**, *16*, 1440–1444.
- (77) Gao, Y.; Kuang, Y.; Guo, Z.-F.; Guo, Z.; Krauss, I. J.; Xu, B. Enzyme-Instructed Molecular Self-Assembly Confers Nanofibers and a Supramolecular Hydrogel of Taxol Derivative. *J. Am. Chem. Soc.* **2009**, *131*, 13576–13577.
- (78) Zhou, J.; Du, X.; Yamagata, N.; Xu, B. Enzyme-Instructed Self-Assembly of Small D-Peptides as a Multiple- Step Process for Selectively Killing Cancer Cells. *J. Am. Chem. Soc.* **2016**, *138*, 3813–3823.
- (79) Wang, H.; Feng, Z.; Wang, Y.; Zhou, R.; Yang, Z.; Xu, B. Integrating Enzymatic Self-Assembly and Mitochondria Targeting for Selectively Killing Cancer Cells without Acquired Drug Resistance. *J. Am. Chem. Soc.* **2016**, *138*, 16046–16055.
- (80) Kalafatovic, D.; Nobis, M.; Javid, N.; Frederix, P. W. J. M.; Anderson, K. I.; Saunders, B. R.; Ulijn, R. V. MMP-9 Triggered Micelle-to-Fibre Transitions for Slow Release of Doxorubicin. *Biomater. Sci.* **2015**, *3*, 246–249.
- (81) Kalafatovic, D.; Nobis, M.; Son, J.; Anderson, K. I.; Ulijn, R. V. MMP-9 Triggered Self-Assembly of Doxorubicin Nanofiber Depots Halts Tumor Growth. *Biomaterials* **2016**, *98*, 192–202.

- (82) Tung, C.-H.; Bredow, S.; Mahmood, U.; Weissleder, R. Preparation of a Cathepsin D Sensitive Near-Infrared Fluorescence Probe for Imaging. *Bioconjugate Chem.* **1999**, *10*, 892–896.
- (83) Medintz, I. L.; Clapp, A. R.; Brunel, F. M.; Tiefenbrunn, T.; Tetsuo Uyeda, H.; Chang, E. L.; Deschamps, J. R.; Dawson, P. E.; Mattoussi, H. Proteolytic Activity Monitored by Fluorescence Resonance Energy Transfer through Quantum-Dot-peptide Conjugates. *Nat. Mater.* **2006**, *5*, 581–589.
- (84) Burgess, L.; Chen, J.; Wolter, N. E.; Wilson, B.; Zheng, G.; Ramanujam, N.; Mitchell, M. F.; Mahadevan, A.; Warren, S.; Thomsen, S.; Silva, E.; Richards-Kortum, R.; Lam, S.; Kennedy, T.; Unger, M.; Miller, Y. E.; Gelmont, D.; Rusch, V.; Gipe, B.; Howard, D.; LeRiche, J. C.; Coldman, A.; Gazdar, A. F.; Jayaprakash, V.; Sullivan, M.; Merzianu, M.; Rigual, N. R.; Loree, T. R.; Popat, S. R.; Moysich, K. B.; Ramananda, S.; Johnson, T.; Marshall, J. R.; Hutson, A. D.; Mang, T. S.; Wilson, B. C.; Gill, S. R.; Frustino, J.; Bogaards, A.; Reid, M. E.; Poh, C. F.; Ng, S. P.; Williams, P. M.; Zhang, L.; Laronde, D. M.; Lane, P.; Macaulay, C. Topical MMP Beacon Enabled Fluorescence-Guided Resection of Oral Carcinoma. *Opt. Soc. Am.* **2016**, *7*, 1089–1099.
- (85) Chi, C.; Du, Y.; Ye, J.; Kou, D.; Qiu, J.; Wang, J.; Tian, J.; Chen, X. Intraoperative Imaging-Guided Cancer Surgery: From Current Fluorescence Molecular Imaging Methods to Future Multi-Modality Imaging Technology. *Theranostics* **2014**, *4*, 1072–1084.
- (86) Kim, K.; Lee, M.; Park, H.; Kim, J.-H.; Kim, S.; Chung, H.; Choi, K.; Kim, I.-S.; Seong, B. L.; Kwon, I. C. Cell-Permeable and Biocompatible Polymeric Nanoparticles for Apoptosis Imaging. *J. Am. Chem. Soc.* **2006**, *128*, 3490–3491.
- (87) Lee, S.; Cha, E.-J.; Park, K.; Lee, S.-Y.; Hong, J.-K.; Sun, I.-C.; Kim, S. Y.; Choi, K.; Kwon, I. C.; Kim, K.; Ahn, C.-H. A Near-Infrared-Fluorescence-Quenched Gold-Nanoparticle Imaging Probe for In Vivo Drug Screening and Protease Activity Determination. *Angew. Chem.* **2008**, *120*, 2846–2849.
- (88) Matsuo, K.; Kamada, R.; Mizusawa, K.; Imai, H.; Takayama, Y.; Narazaki, M.; Matsuda, T.; Takaoka, Y.; Hamachi, I. Specific Detection and Imaging of Enzyme Activity by Signal-Amplifiable Self-Assembling (19)F MRI Probes. *Chem. - Eur. J.* **2013**, *19*, 12875–12883.
- (89) Yang, K.; Zhu, L.; Nie, L.; Sun, X.; Cheng, L.; Wu, C.; Niu, G.; Chen, X.; Liu, Z. Visualization of Protease Activity In Vivo Using an Activatable Photo-Acoustic Imaging Probe Based on CuS Nanoparticles. *Theranostics* **2014**, *4*, 134–141.
- (90) Jiang, T.; Olson, E. S.; Nguyen, Q. T.; Roy, M.; Jennings, P. A.; Tsien, R. Y. Tumor Imaging by Means of Proteolytic Activation of Cell-Penetrating Peptides. *Proc. Natl. Acad. Sci. U. S. A.* **2004**, *101*, 17867–17872.
- (91) Dubikovskaya, E. A.; Thorne, S. H.; Pillow, T. H.; Contag, C. H.; Wender, P. A. Overcoming Multidrug Resistance of Small-Molecule Therapeutics through Conjugation with Releasable Octaarginine Transporters. *Proc. Natl. Acad. Sci. U. S. A.* **2008**, *105*, 12128–12133.
- (92) Shapira, A.; Livney, Y. D.; Broxterman, H. J.; Assaraf, Y. G. Nanomedicine for Targeted Cancer Therapy: Towards the Overcoming of Drug Resistance. *Drug Resist. Updates* **2011**, *14*, 150–163.
- (93) Olson, E. S.; Aguilera, T. A.; Jiang, T.; Scadeng, M.; Nguyen, Q. T.; Ellies, L. G.; Tsien, R. Y. In Vivo Characterization of Activatable Cell Penetrating Peptides for Targeting Protease Activity in Cancer. *Proc. Natl. Acad. Sci. U. S. A.* **2010**, *107*, 4317–4322.
- (94) Olson, E. S.; Jiang, T.; Aguilera, T. A.; Nguyen, Q. T.; Ellies, L. G.; Scadeng, M.; Tsien, R. Y. Activatable Cell Penetrating Peptides Linked to Nanoparticles as Dual Probes for in Vivo Fluorescence and MR Imaging of Proteases. *Proc. Natl. Acad. Sci. U. S. A.* **2010**, *107*, 4311–4316.
- (95) Whitney, M.; Savariar, E. N.; Friedman, B.; Levin, R. A.; Crisp, J. L.; Glasgow, H. L.; Lefkowitz, R.; Adams, S. R.; Steinbach, P.; Nashi, N.; Nguyen, Q. T.; Tsien, R. Y. Ratiometric Activatable Cell-Penetrating Peptides Provide Rapid in Vivo Readout of Thrombin Activation. *Angew. Chem., Int. Ed.* **2013**, *52*, 325–330.
- (96) Hua, N.; Baik, F.; Pham, T.; Phinikaridou, A.; Giordano, N.; Friedman, B.; Whitney, M.; Nguyen, Q. T.; Tsien, R. Y.; Hamilton, J. A. Identification of High-Risk Plaques by MRI and Fluorescence Imaging in a Rabbit Model of Atherothrombosis. *PLoS One* **2015**, *10*, e0139833.
- (97) Crisp, J. L.; Savariar, E. N.; Glasgow, H. L.; Ellies, L. G.; Whitney, M. A.; Tsien, R. Y. Dual Targeting of Integrin $\alpha v \beta 3$ and Matrix Metalloproteinase-2 for Optical Imaging of Tumors and Chemotherapeutic Delivery. *Mol. Cancer Ther.* **2014**, *13*, 1514–1525.
- (98) Blum, G.; Mullins, S. R.; Keren, K.; Fonovič, M.; Jedeszko, C.; Rice, M. J.; Sloane, B. F.; Bogoy, M. Dynamic Imaging of Protease Activity with Fluorescently Quenched Activity-Based Probes. *Nat. Chem. Biol.* **2005**, *1*, 203–209.
- (99) Whitley, M. J.; Cardona, D. M.; Lazarides, A. L.; Spasojevic, I.; Ferrer, J. M.; Cahill, J.; Lee, C.-L.; Snuderl, M.; Blazer, D. G.; Hwang, E. S.; Greenup, R. A.; Mosca, P. J.; Mito, J. K.; Cuneo, K. C.; Larrier, N. A.; O'Reilly, E. K.; Riedel, R. F.; Eward, W. C.; Strasfeld, D. B.; Fukumura, D.; Jain, R. K.; Lee, W. D.; Griffith, L. G.; Bawendi, M. G.; Kirsch, D. G.; Brigman, B. E. A Mouse-Human Phase I Co-Clinical Trial of a Protease-Activated Fluorescent Probe for Imaging Cancer. *Sci. Transl. Med.* **2016**, *8*, 320ra4.
- (100) Lock, L. L.; Cheetham, A. G.; Zhang, P.; Cui, H. Design and Construction of Supramolecular Nanobeacons for Enzyme Detection. *ACS Nano* **2013**, *7*, 4924–4932.
- (101) Lock, L. L.; Reyes, C. D.; Zhang, P.; Cui, H. Tuning Cellular Uptake of Molecular Probes by Rational Design of Their Assembly into Supramolecular Nanoprobes. *J. Am. Chem. Soc.* **2016**, *138*, 3533–3540.
- (102) Yang, L.; Peng, X.-H.; Wang, Y. A.; Wang, X.; Cao, Z.; Ni, C.; Karna, P.; Zhang, X.; Wood, W. C.; Gao, X.; Nie, S.; Mao, H. Receptor-Targeted Nanoparticles for In Vivo Imaging of Breast Cancer. *Clin. Cancer Res.* **2009**, *15*, 4722–4732.
- (103) Law, B.; Weissleder, R.; Tung, C.-H. Protease-Sensitive Fluorescent Nanofibers. *Bioconjugate Chem.* **2007**, *18*, 1701–1704.
- (104) Malik, R.; Qian, S.; Law, B. Design and Synthesis of a near-Infrared Fluorescent Nanofiber Precursor for Detecting Cell-Secreted Urokinase Activity. *Anal. Biochem.* **2011**, *412*, 26–33.
- (105) Lowe, S. B.; Dick, J. A. G.; Cohen, B. E.; Stevens, M. M. Multiplex Sensing of Protease and Kinase Enzyme Activity via Orthogonal Coupling of Quantum Dot-Peptide Conjugates. *ACS Nano* **2012**, *6*, 851–857.
- (106) Ye, D.; Shuhendler, A. J.; Cui, L.; Tong, L.; Tee, S. S.; Tikhomirov, G.; Felsher, D. W.; Rao, J. Bioorthogonal Cyclization-Mediated in Situ Self-Assembly of Small-Molecule Probes for Imaging Caspase Activity in Vivo. *Nat. Chem.* **2014**, *6*, 519–526.
- (107) Ye, D.; Shuhendler, A. J.; Pandit, P.; Brewer, K. D.; Tee, S. S.; Cui, L.; Tikhomirov, G.; Rutt, B.; Rao, J. Caspase-Responsive Smart Gadolinium-Based Contrast Agent for Magnetic Resonance Imaging of Drug-Induced Apoptosis. *Chem. Sci.* **2014**, *5*, 3845–3852.
- (108) Palmer, M.; Shen, B.; Jeon, J.; Lin, J.; Chin, F. T.; Rao, J. Preclinical Kinetic Analysis of the Caspase-3/7 PET Tracer 18F-C-SNAT: Quantifying the Changes in Blood Flow and Tumor Retention After Chemotherapy. *J. Nucl. Med.* **2015**, *56*, 1415–1421.
- (109) Witney, T. H.; Hoehne, A.; Reeves, R. E.; Ilovich, O.; Namavari, M.; Shen, B.; Chin, F. T.; Rao, J.; Gambhir, S. S. A Systematic Comparison of 18F-C-SNAT to Established Radiotracer Imaging Agents for the Detection of Tumor Response to Treatment. *Clin. Cancer Res.* **2015**, *21*, 3896–3905.
- (110) Nejadnik, H.; Ye, D.; Lenkov, O. D.; Donig, J. S.; Martin, J. E.; Castillo, R.; Derugin, N.; Sennino, B.; Rao, J.; Daldrup-Link, H. Magnetic Resonance Imaging of Stem Cell Apoptosis in Arthritic Joints with a Caspase Activatable Contrast Agent. *ACS Nano* **2015**, *9*, 1150–1160.
- (111) Gao, W.; Xiang, B.; Meng, T.; Liu, F.; Qi, X. Chemotherapeutic Drug Delivery to Cancer Cells Using a Combination of Folate Targeting and Tumor Microenvironment-Sensitive Polypeptides. *Biomaterials* **2013**, *34*, 4137–4149.
- (112) Yu, H.; Chen, J.; Liu, S.; Lu, Q.; He, J.; Zhou, Z.; Hu, Y. Enzyme Sensitive, Surface Engineered Nanoparticles for Enhanced Delivery of Camptothecin. *J. Controlled Release* **2015**, *216*, 111–120.

(113) Ruan, S.; Cao, X.; Cun, X.; Hu, G.; Zhou, Y.; Zhang, Y.; Lu, L.; He, Q.; Gao, H. Matrix Metalloproteinase-Sensitive Size-Shrinkable Nanoparticles for Deep Tumor Penetration and pH Triggered Doxorubicin Release. *Biomaterials* **2015**, *60*, 100–110.

(114) Zhong, J.; Li, L.; Zhu, X.; Guan, S.; Yang, Q.; Zhou, Z.; Zhang, Z.; Huang, Y. A Smart Polymeric Platform for Multistage Nucleus-Targeted Anticancer Drug Delivery. *Biomaterials* **2015**, *65*, 43–55.

(115) Ku, T.-H.; Chien, M.-P.; Thompson, M. P.; Sinkovits, R. S.; Olson, N. H.; Baker, T. S.; Gianneschi, N. C. Controlling and Switching the Morphology of Micellar Nanoparticles with Enzymes. *J. Am. Chem. Soc.* **2011**, *133*, 8392–8395.

(116) Stefflova, K.; Chen, J.; Marotta, D.; Li, H.; Zheng, G. Photodynamic Therapy Agent with a Built-In Apoptosis Sensor for Evaluating Its Own Therapeutic Outcome in Situ. *J. Med. Chem.* **2006**, *49*, 3850–3856.

(117) Stefflova, K.; Chen, J.; Li, H.; Zheng, G. Targeted Photodynamic Therapy Agent with a Built-In Apoptosis Sensor for In Vivo Near-Infrared Imaging of Tumor Apoptosis Triggered by Its Photosensitization In Situ. *Mol. Imaging* **2006**, *5*, 520–532.

(118) Zheng, G.; Chen, J.; Stefflova, K.; Jarvi, M.; Li, H.; Wilson, B. C. Photodynamic Molecular Beacon as an Activatable Photosensitizer Based on Protease-Controlled Singlet Oxygen Quenching and Activation. *Proc. Natl. Acad. Sci. U. S. A.* **2007**, *104*, 8989–8994.

(119) Liu, T. W.; Akens, M. K.; Chen, J.; Wise-Milestone, L.; Wilson, B. C.; Zheng, G. Imaging of Specific Activation of Photodynamic Molecular Beacons in Breast Cancer Vertebral Metastases. *Bioconjugate Chem.* **2011**, *22*, 1021–1030.

(120) Liu, T. W.; Akens, M. K.; Chen, J.; Wilson, B. C.; Zheng, G. Matrix Metalloproteinase-Based Photodynamic Molecular Beacons for Targeted Destruction of Bone Metastases in Vivo. *Photochem. Photobiol. Sci.* **2016**, *15*, 375–381.

(121) Yi, D. K.; Sun, I.; Ryu, J. H.; Koo, H.; Park, C. W.; Youn, I.; Choi, K.; Kwon, I. C.; Kim, K.; Ahn, C. Matrix Metalloproteinase Sensitive Gold Nanorod for Simultaneous Bioimaging and Photothermal Therapy of Cancer. *Bioconjugate Chem.* **2010**, *21*, 2173–2177.

(122) Yang, Y.; Aw, J.; Chen, K.; Liu, F.; Padmanabhan, P.; Hou, Y.; Cheng, Z.; Xing, B. Enzyme-Responsive Multifunctional Magnetic Nanoparticles for Tumor Intracellular Drug Delivery and Imaging. *Chem. - Asian J.* **2011**, *6*, 1381–1389.

(123) Lock, L. L.; Tang, Z.; Keith, D.; Reyes, C.; Cui, H. Enzyme-Specific Doxorubicin Drug Beacon as Drug-Resistant Theranostic Molecular Probes. *ACS Macro Lett.* **2015**, *4*, 552–555.

(124) Ansari, C.; Tikhomirov, G. A.; Hong, S. H.; Falconer, R. A.; Loadman, P. M.; Gill, J. H.; Castaneda, R.; Hazard, F. K.; Tong, L.; Lenkov, O. D.; Felsner, D. W.; Rao, J.; Daldrup-Link, H. E. Development of Novel Tumor-Targeted Theranostic Nanoparticles Activated by Membrane-Type Matrix Metalloproteinases for Combined Cancer Magnetic Resonance Imaging and Therapy. *Small* **2014**, *10*, 566–575.

(125) Lee, G. Y.; Qian, W. P.; Wang, L.; Wang, Y. A.; Staley, C. a.; Satpathy, M.; Nie, S.; Mao, H.; Yang, L. Theranostic Nanoparticles with Controlled Release of Gemcitabine for Targeted Therapy and MRI of Pancreatic Cancer. *ACS Nano* **2013**, *7*, 2078–2089.